ISTANBUL TECHNICL UNIVERSITY ★ GRADUATE SCHOOL OF SCIENCE, ENGINEERING AND TECHNOLOGY

SINGLE PARTICLE IMPEDANCE MEASUREMENTS USING A MICROFLUIDIC CHIP

Master of Science THESIS

Golezar GILANIZADEHDIZAJ

Department of Nanoscience &Nanoengineering

Nanoscience &Nanoengineering Programme

JANUARY 2015

ISTANBUL TECHNICL UNIVERSITY ★ GRADUATE SCHOOL OF SCIENCE, ENGINEERING AND TECHNOLOGY

SINGLE PARTICLE IMPEDANCE MEASUREMENTS USING A MICROFLUIDIC CHIP

Master of Science THESIS

Golezar GILANIZADEHDIZAJ

(513121007)

Department of Nanoscience &Nanoengineering

Nanoscience &Nanoengineering Programme

Thesis Advisor: Assoc. Prof. Dr. Hüseyin KIZIL

15 DECEMBER 2014

İSTANBUL TEKNİK ÜNİVERSİTESİ *FEN BİLİMLERİ ENSTİTÜSÜ

MIKROAKIŞKAN ÇIPLERDE TEK PARÇACIK IMPEDANS ÖLÇÜM SISTEMI TASARIMI

YÜKSEK LİSANS TEZİ

Golezar GILANIZADEHDIZAJ

(513121007)

Nano Bilim ve Nano Mühendisliği Anabilim Dalı

Nano Bilim ve Nano Mühendisliği Programı

Tez Danışmanı: Doç. Dr. Hüseyin KIZIL

15 ARALIK 2014

Golezar GILANIZADEHDIZAJ, a **M.Sc.** student of ITU Graduate School of Science, Engineering and Technology, student ID 513121007, successfully defended the **thesis** entitled "**SINGLE PARTICLE IMPEDANCE MEASUREMENTS USING A MICROFLUIDIC CHIP**", which she prepared after fulfilling the requirements specified in the associated legislations, before the jury whose signatures are below.

Thesis Advisor: Assoc. Prof. Dr. Hüseyin KIZIL ….....

Istanbul Technical University

Jury Members: Assoc. Prof. Dr. Esra Özkan ZAYİM ….....

Istanbul Technical University

Assoc. Prof. Dr. Erdem ALACA ….....

Koç University

Date of Submission: 15 December 2014

Date of Defense: 29 January 2015

Acknowledgement

I would like to express my gratitude to my supervisor Professor Hüseyin Kızıl for the useful comments, remarks and engagement through the learning process of this master thesis as well as for allowing me to use the facilities at ITU Microfluidics Laboratory. Also I would like to thank Emre Altınağaç for introducing me to the topic in the beginning of the way and helping me how to use the equipment. Furthermore my special thanks go to all the group members, who made the months I have spent at ITU too much fun.

Finally I'd like to thank my family and friends who have taught me so much throughout. Without your support, I may not have been able to make it this far. I owe all of you so much and will be grateful forever for your love.

January 2015 **Golezar Gilanizadehdizaj**

TABLE OF CONTENT

LIST OF FIGURES

LIST OF FIGURES continued

LIST OF TABLES

SINGLE PARTICLE IMPEDANCE MEASUREMENTS USING A MICROFLUIDIC CHIP

Summary

In recent years, cancer has become the number one killer in many countries and conventional diagnosis are very invasive, time-consuming, complicated process, and need stringent laboratory conditions. Traditional approaches study a group of cells which the results are averages and cannot exactly show individual cells. Hence single cell analyze is needed to associate cellular events with genomic information and plays an important role in biological measurement and medical research. The so-called “lab-on-a-chip” devices for handling samples in bio fluids are very applicable in biology and chemistry as they have lost of profits such as high resolution, very fast and inexpensive for analyzing and synthesizing and give the opportunity of manipulating of single cells, which is a key technology in cell engineering such as drug injection and gene introduction. For single cell analysis, cell impedance analysis has developed rapidly and has become an effective method of biological measurement. The temperature, electric conductivity and mobility of a cell can influence its impedance characteristics directly or indirectly so the cell impedance characteristic can be used to understand biological characteristic behavior. This Master’s Thesis project presents a microfluidic chip for single-particle impedance measurement. The device with integrated actuation electrodes utilizes the DEP and controlled pressure-driven liquid flows to capture the single particle and sensing electrodes to measures the impedance of particle. The impedance was measured at different voltages ranges (0.1-2 V) between 3 KHz and 500 KHz. The impedance increase can be explained by a gradual blockage of the electrical path between the sensing electrodes. The impedance measurement over wide frequency range revealed that the impedance decreased as the frequency increased because of the double-layer capacitance on each electrode. In addition, the increment ratio was more evident for the particle experiment at the low frequency. Also it is obvious that with increasing the voltage, it was a slight decrease in impedance in most of frequencies. Furthermore comparison of the obtained results for DI water and 150mM NaCl shows less impedance magnitudes for 150mM NaCl which can be described due to increase of the conductivity of the suspending medium. The mean of impedance increased in DI water is 10.13% and in Nacl is 10.20%. Although different solutions are used for impedance evaluation of polystyrene particles, results in both case are close to each other with approximately 10% increasing.

MIKROAKIŞKAN ÇIPLERDE TEK PARÇACIK IMPEDANS ÖLÇÜM SISTEMI TASARIMI

Özet

Son yıllarda, kanser hastalığı dunyada, birçok ülkede, en önemli ölüme nedeni olan hastalıklardan birisidir. Geleneksel tanıların yöntemleri zaman alıcı, karmaşık süreç ve ayrıca sıkı laboratuvar koşulları gerektirir. Klasik yaklaşımlarda, hücrelerin çoğalmasını, farklılaşma, protein veya gen ekspresyonu, ilaç tepkisi ve toksisite deneyleri gibi özelikleri anlamak için, hücreleri grup olarak gözönüne alıp ve incelemek yaygın olarak kullanılmaktadır.

Bir hücre grubu tarafından tarif edilen hücre parametreleri, hücre gruplarından elde edilmiş ve ortalama olarak gösterilebilir, ancak tam olarak tek tek hücrelerin özelliklerini gösteremez. Üstelik, heterojenlik hücrelerinin popülasyonda tahmin edilemez. Bu nedenle karmaşık hücresel prosedürü anlamak için ve genomik bilgi hücresel olayları anlamak için tek hücreli analiz gerekmektedir. Bu analiz, biyolojik ölçümlerde ve tibbi araştırmada önemli olduğu gösterilmektedir.

Bu çalışmada biyo sıvı numuneleri ele alma amacıyla, MEMS teknikleri ile "lab-on-a-chip" adlanan cihazlar imal edilmiştir. Biyo sıvı numunelerin ele alınması biyoloji ve kimyada çok uygulanabilir. Buda, yüksek çözünürlüklü, çok hızlı ve ucuz analiz ve sentez gibi faydalara neden olmaktadır. Ayrıca, tek hücre manipüle fırsatı verir. Bu cihazlar ilaç enjeksiyonu ve gen tanıtımı gibi amaçlarda hücre mühendisliğinde önemli bir teknolojidir. Mekanik, optik, biyo-kimyasal ve elektriksel teknikler gibi yongaları üzerinde hücrelerin manipüle edilmesi için kullanılan çeşitli yaklaşımlar vardır. Elektrik tekniği veya elektrokınetik (DC / AC), avantajlı özelliklere sahiptir. Onlar biyo-hedeflere karşın, temassızlardır. Elektrik tekniği veya elektrokınetik (DC / AC) parçacıkların kontrol etmek için, bir elektrik alanının gradyanı kuvvetini kullanılmaktadır (ya da elektrik neden olduğu ve yardımı ile sıvı ile aynı anda akar). Böylece hücrelerein deforme ve invaziv zararını önlemektedir.

Son birkaç yıl içinde, elektrokinetik akım alternativi (ACEK, ana güç girişi olarak alternatif akım kullanılarak) araştırmacıların ilgisini kazanmaktadır. Buda mikroakışkan hareketi için büyük bir potansiyel göstermiştir. Bir üniform olmayan elektrik alanı, süspansiyon ortamında polarize parçacık ve sonraki asimetrik elektrik kuvveti eylemleri ile etkileşimeye girebilir. Buna dielektroforez denir (DEP) (Pohl and Pollock, 1978). Bu teknik, tutucu, manipüle ve hücreler, virüsler, proteinler ve DNA gibi bioparticles ayrılması gibi biyolojik işlemlerde önemli bir uygulama alanı vardır.

Yüksek frekanslı AC alanları (> 100 kHz) kullanarak DEP yöntemine göre hücre tutması için birçok faydası vardır. Böylece, elektroliz ve elektrot-elektrolit arayüzleri kimyasal reaksiyonlarını en aza indirir. Ayrıca, biyolojik hücrelerin membran

şarjının azaltılması ve elektrikli kontrol ederek, birkaç saniye içinde tek veya küme hücrelerin tam manipülasyonun yapılması gibi faydalara neden olmaktadır.

Iki türlü DEP kuvvetleri bulunmaktadır, pozitif DEP (pDEP) ve negatife DEP (nDEP). Pozitif DEP (pDEP) parçacıkları model verilmiş elektrotlar doğrusunda çekmektedir, buda hücre liziz sorununa neden olmaktadır. Negatife DEP (nDEP) parçacıkları istenmeyen birleştirme bölgeden itmektedir.

Son zamanlarda, negatif DEP kullanan tek hücrelerinin aktif pozisyon kontrolü, yüksek verimli, tek hücreli izolasyonu için geliştirilmiştir. Ayrıca, mikroakışkan cihazları hücre esaslı tahliller için geliştirilmiştir. Pozitif DEP (pDEP) ile negatife DEP (nDEP) karşılaştırılmasında, yaygın olarak kullanılan hücre kültür ortamında, sadece nDEP süspansiyon halinde olan hücrelerle yapılabilir. Oysa. hücreler bulunan ortama göre daha polarize olduğunu garanti etmek için pDEP, düşük iletkenliğe sahip ortam içinde yapılmalıdır.

Tek hücre analizi için, hücre impedans analizi hızla geliştirilmiştir, ayrıca biyolojik ölçümünde etkili bir yöntem haline gelmiştir. Bir hücrenin sıcaklığı, elektrik iletkenliği ve hareket, doğrudan ya da dolaylı olarak impedans özelliklerini etkileyebilir. Bu nedenle, Hücre impedans karakteristiği biyolojik karakteristik davranışlarını anlamak için

kullanılabilir. Tek hücreleri üzerinde ölçümler patolojik dokulara göre elektriksel özellikleri hakkında daha doğru bilgi sağlamaktadır.

Bu projenin amacı, solüsyondan tek bir parçacık yakalamak ve parçacığın özellikleri hakkında bilgi almak için bunun empedans ölçümünü almaktır. Bu hedefe, Ledit (V13) kullanılarak elektrotlar ve mikrokanal yapıları tasarlanmıştır ve bunların her biri için lazer yazar kullanarak maske tasarlanmıştır. Cam kalıbı üzerine elektrotlar elde etmek için standart photolithograpy teknolojisi ve kaldırma süreci kullanılmaktadır. Bu çalışmada Titanyum olan metal tabaka cam alt-tabaka üzerinde elektron akımı fiziksel buhar depozisyonu ile tevdilmiştir. Kanal bölgesini tanımlamak için fotolitografi kullanımıyla, mikrokanal için bir Poli-di-metil-siloksan (PDMS) çip oluşturulmuştur. Sonra PDMS yapılarak, kalıp yapısı içine dökülüp, sertleştirilmiş ve nihayet alt tabaka kalıbidan soyulmuştur. Yüzey işlemini oksijen plazma temizleyici kullanarak yapıldıktan sonra, tamamlanan PDMS yapısı cam tabanı ile birleştirilmiştir. Çip yakalama boşlukları, ana kanal, DEP veya harekete geçirme elektrotlar, ve hassas elektrotlardan oluşmaktadır.

İlk olarak, parçacıklar girişiden içeri alınır ve ana kanal üzerinden hareket eder. Bir parçacık harekete geçiren elektrotlara geldiğinde, negatif DEP etkisinden dolayı yakalama boşlukları tarafına hareket eder. Empedans tespiti elektrot tepkisi periyodik alternatif akım (AC) sinyalinin uygulanması ile ilişkilidir. Empedans tespıtı solüsyonda parçacık olmadan ve bir parçacık ile, her iki durumda hassas elektrotlarla ölçülmektedir. Daha sonra, iki hassas elektrotlar arasında parçacık yakalandıktan sonra empedans değişikliği ölçülmesi sağlanmaktadır. Yakalama boşluklarında yerleştirilen drenaj kanalı ve hassas elektrotlar, parçacığı istenen yerlere izolasyon edmesini sağlamaktadir.

Bu Yüksek Lisans tezi projesi mikroakışkan cihazı veya lab-on-a-chip tek parçacık impedans ölçümü üzerine yapılmıştır. Geliştirilen cihaz, tek bir parçacığı tuzaklaması için geliştirilmiştir. Tek bir parçacığı tuzaklamak için nDEP elektrotlarını entegre çalıştırarak ve sıvı akışlarını basınç odaklı kontrol ederker gerçekleştirilmiştir. Ayrıca, geliştirilen cihaz, duyarlı elektrotları kullanarak hücrenin impedans ölçmek için kullanılmıştır. Önerilen teknik, çeşitli kanser hücrelerinin ayırt edebilir.

Empedans farklı voltaj aralıklarında (0,1-2 V) ve 3 KHz ve 500 KHz frekanslar aralığında ölçülmektedir. Empedans artışı hassas elektrotlar arasındaki elektrik yolu tedricen bloke edilmesiyle izah edilebilir.

Geniş bir frekans aralığında empedans olçümünde, her elektrot çift tabakalı kapasitesii olduğuna göre, frekans arttıkça empedans azaldığını göstermektedir.

Ayrıca, parçacık deneylerinde, bu artış oranı düşük frekanslarda daha belirgindi. Buna ek olarak, artan voltajlarda, frekansların çoğunda empedansın hafif bir azalması görulmektedir. DI su ve 150 mM NaCl için elde edilen sonuçların karşılaştırmasına göre 150 mM NaCl daha az empedans büyüklüğünü göstermektedir.

Bu özellik, süspansiyon ortamının iletkenliği artışı ile tanımlanabilir. DI su'da artan empedans ortalamasi 10.13% ve NaCl'de 10.20% 'dir. Polistiren taneciklerin empedans değerlendirme için farklı solüsyonlar kullanılmiştır, ancak her iki durumda'da empedans artışında sonuçlar birbirine yakındır (10%).

1. INTRODUCTION

1.1 Background and Motivation

In recent years, cancer has become the number one killer in many countries. Because of improvements in health care practices and advances in medical science chronic diseases such as cancer, heart disease, cerebrovascular disease, and so forth, the average life-span of human continues to increase in most parts of the world. However, breast cancer and cervical cancer are the most common types of cancer affecting women. Many cancer patients already have long-distance metastases upon diagnosis and a large percentage of these patients develop metastatic diseases following surgical removal of the primary tumor. Medical steps are taken either to prevent the development of a disease (primary prophylaxis) or to arrest its further development in the event that it has already been developed (secondary prophylaxis). Clearly, the effectiveness of secondary prophylaxis measures is dependent on the timeliness with which the disease is detected, and thus sophisticated methods are required to detect the presence of possible cellular disorders at the very earliest stages of the disease's incubation period. In general, the cancer diseases is diagnosed using a combination of surgical biopsy, radiological, and pathological assessment of tissue samples based on the morphological and immunohistochemical characteristics. However, the manner of diagnosis is invasive, time-consuming, complicated process, and need stringent laboratory conditions. Hence, development of cancer detection methods that are much more reliable, minimally invasive, inexpensive and easy to use is still required.

1.2 Introduction to Single Cell Capture

Traditional approaches study a group of cells in order to understand cell proliferation, differentiation, protein or gene expression, drug response and toxicity

assays and cell parameters described by a group of cell are averages and cannot exactly show individual cells. Furthermore, heterogeneity cannot be estimated in a population of cells. Hence for understanding complicated cellular procedure, single cell analyze is needed to associate cellular events with genomic information and plays an important role in biological measurement and medical research. (Fortina et al., 2002; Graf and Stadtfeld 2008; Irish et al. 2006). In addition, analyzing individual cells with higher spatiotemporal resolutions will provide more accurate representation of cell-to-cell variation in an isogenic population instead of the stochastic average masked by bulk measurements. (Wang and Bodovitz, 2010).

The so-called "lab-on-a-chip" devices fabricated with MEMS techniques (Gawad et al., 2004) for handling samples in bio fluids are very applicable in biology and chemistry as they have lost of profits such as high resolution, very fast and inexpensive for analyzing and synthesizing and give the opportunity of manipulating of single cells, which is a key technology in cell engineering such as drug injection and gene introduction where no agent elaboration is needed. (Fortina et al., 2002).

There are several approaches being used for manipulating cells on chips, and generally can be classified into following categories based on the utilized driving force. The first one is the mechanical technique using a microtweezer or micropipette, which requires highly sophisticated skill to handle a cell as small as 10 μm in diameter (Hochmuth, 2000); or loading cells into mechanical structures like microwells/cavities (Revzin et al, 2005; Wu et al., 2008), or micropillars (Jang and Wang, 2007) but it needs waiting and has the restriction of cell proliferation. The second one is the optical technique known as optical/laser manipulation, like optical tweezers and dynamic holographic optical tweezers (Curtis et al. 2002), which can catch a cell with good accuracy (Ashkin et al., 1990). However, these often required high optical power level (1 mW - 100 mW), which may cause damage to the particles due to local heating or two photon absorption (Wu et al., 2008) and the system used for the laser manipulation is relatively large and expensive. The third one is the bio-chemical technique, which patterns the substrate with materials that support and/or resist cell adhesion such as the specific binding between antibodies and cells through one coating layer of Self-assembled monolayers (SAMs) on the substrate (Le Pioufle et al., 2000). The forth one is the electrical technique or electrokinetics (in DC/AC), which utilizes the gradient force of an electric field, to

control/pattern the particles (or with the aid of electricity-caused fluid flows simultaneously). Among these techniques, immobilizing cells at certain sites in electrical approaches has the advantageous features that they are contact-free against the bio-targets, thus avoiding directly deforming and doing invasive harm to the cells; they enable electrical addressing of sites where cells are held (Taff and Voldman, 2005), allowing for the easy integration of electrical detection of cell products and/or electrical stimulation of particular cells. Moreover, electrical approaches are flexible, that is, they can also be combined with the first three approaches to make trapping more efficient (Muys et al., 2005; Hunt and Westervelt, 2006; Suehiro et al., 2006).

In the last few years, alternating current electrokinetics (ACEK, using alternating current as the main power input) receives increasing research interest as it has demonstrated great potential for microfluidic actuation (Ramos et al., 1998). A nonuniform electric field can interact with the polarizable particle in the suspending medium and the subsequent asymmetric action of the electrical force on a particle. This phenomenon is called dielectrophoresis (DEP) (Pohl and Pollock, 1978). This technique has vital applications in biological procedures, such as trapping, manipulating and separating bioparticles like cells, viruses, proteins and DNA (Bakewell et al., 1998; Yang et al., 2000). Using high-frequency AC fields (>100 kHz) has several beneficial features for DEP-based cellular traps. First, operating at such frequencies minimizes electrolysis and chemical reactions at electrode-electrolyte interfaces, where cause gas formation and raise difficulty in observation. Second, it reduces membrane charging of biological cells (Jones, 2005). Membrane charging is due to the potential developed across cell membranes in electric fields. This potential, which can impact cell physiology, can be diminished by applying of high-frequency fields. Third, a precise manipulation of cells for single or in cluster can be realized in a few seconds by controlling the electric field without a mechanical moving part. The magnitude of the DEP force varies depending on the input voltage and frequency that we can control. In addition, such operation further allows electrical measurements of the properties of captured and assembled particles (Lennon et al., 2006; Kwong et al., 2005).

There are two kinds of DEP forces, which can pull particles toward the patterned electrodes [positive DEP (pDEP)], which results in a cell lysis problem or push cells from the undesired assembling region [negative DEP (nDEP)]. Recently, active positioning control of single cells using negative DEP has been developed for high-throughput single-cell isolation and microfluidic chips for cell-based assays. In contrast to pDEP, which must be performed in media with low conductivity to guarantee that the cells are more polarizable than the media, only nDEP can be performed with cells suspended in commonly used cell culture media. Because these media have higher conductivity and relative permittivity than cells. Prior nDEP traps include nDEP quadrupoles (Heida et al., 2001; Voldman et al., 2001), nDEP octopoles (Schnelle et al., 1993), nDEP cages (Manaresi et al., 2003; Yasukawa et al., 2007), and nDEP posts (Voldman et al., 2003).

1.3 Cell Impedance Analysis

For single cell analysis, cell impedance analysis (Rosenthal, and Voldman, 2005), is an effective method which has developed rapidly and has become an effective method of biological measurement. The temperature, electric conductivity and mobility of a cell can influence its impedance characteristics directly or indirectly so the cell impedance characteristic can be used to understand biological characteristic behavior. Measurements on single cells also provide more accurate and in-depth information about electrical properties than do those of pathological tissues. Single-cell impedance also can be applied to study the effect of pharmaceutical compounds (Ye et al., 2003), the effect of viral and bacterial infections (Niikura et al., 2004), and environmental parameters (Gilchrist et al., 2005), toxicity (Giaever and Keese, 1992) and other factors. For the purpose of electrical characterization and sorting of cells, there are several reports about on-chip integration of microfluidics and electrodes (Zou et al., 2008; Sabounchi et al., 2008; Ichiki et al., 2002; Hong et al., 2012; Suehiro et al., 2003; Chen et al., 2014). Recently, Ferrier et al. demonstrated a microfluidic chip with interdigitated electrodes in a microfluidic channel that simultaneously actuates and detects individual biological cells (Ferrier et al., 2008 &2009).

1.4 Organization of the Dissertation

This study presents a microfluidic chip for single-polystyrene impedance measurement. The chip with integrated actuation electrodes utilizes the DEP and controlled pressure-driven liquid flows to capture the single particle and sensing electrodes to measures the impedance of particle. The proposed chip can also be used for single cell and distinguish the various kinds of cancer cells. Additionally, an equivalent circuit model is established. The content of this dissertation is divided into five chapters:

Chapter 1 introduces the importance and variety methods of cell capture through MEMS technology. Measurements on single cells also provide more accurate and in-depth information about electrical properties than do those of pathological tissues.

Chapter 2 introduces DEP theory of the designed microelectrodes. Also an electrical–biological-circuit system is explained.

Chapter 3 presents the fabrication of microelectrodes through MEMS processes, including lithography, deposition and lifting off as well as fabrication of the microchannel. The experimental setup is also shown here.

Chapter 4 demonstrates the measured electrical impedance spectrums of the polystyrene particle at different voltages in different solutions.

Chapter 5 gives some conclusions on this dissertation and application for further biological use.

2. ELECTRICAL MODELING OF THE SYSTEM

In this thesis, we measure the impedance of single particle with the microfluidic chip which contains actuation electrodes used to manipulate a microbead by dielectrophoresis and sensing electrodes to detect the trapping by using the impedance detection method. Combining deflective dielectrophoretic barriers with controlled drag force allows the accurate control of a microbead in suspensions.

2.1 DEP Forces

The DEP was first discovered by Pohl (1951), who then published the governing theory in 1978, which stated that "the motion of suspended particles relative to that of the solvent resulting from polarization forces produced by an inhomogeneous electric field." Since then, DEP has been used in numerous applications such as trapping, levitation, separation and manipulation of latex beads, biological cells, bacteria, virus, proteins and DNA, at micron and sub-micron scales (Bakewell et al., 1998; Yang et al., 2000).

2.1.1 Positive and negative DEP forces

The time-averaged dielectrophoretic force F_{DEP}, exerted on a spherical particle suspended in a dielectric fluid medium and exposed to a non uniform AC electric field can be written as (Pohl and Pollock, 1978):

$$\left\langle \vec{F}_{DEP} \right\rangle = 2\pi a^3 \varepsilon_m \,\mathrm{Re}\left[\underline{K}(\omega) \right] \nabla E_{rms}{}^2 \qquad (2.1)$$

where a is the particle radius, ε_m is the permittivity of the suspension medium, E_{rms} is the root-mean-square (rms) electric field, ∇ is the del vector operator, and $\mathrm{Re}\left[\underline{K}(\omega)\right]$ is the real part of the Clausius-Mossotti factor (CM factor, f_{CM}). CM factor is a parameter of the effective Polariability of the particle which varies as a function of the frequency of the applied field, and the dielectric properties of the particle and the surrounding medium. CM factor is given by

$$\underline{K}(\omega) = \left(\frac{\varepsilon_p^* - \varepsilon_m^*}{\varepsilon_p^* + 2\varepsilon_m^*} \right) \tag{2.2}$$

$$\text{where } \varepsilon_p^* = \varepsilon_p - j\frac{\sigma_p}{\omega} \text{ , } \varepsilon_m^* = \varepsilon_m - j\frac{\sigma_m}{\omega} \tag{2.3}$$

ε_p* and ε_m* are the complex permittivity of the particle and the medium respectively, σ_p and σ_m are the conductivity of the particle and the medium respectively, and ω is the angular frequency of the applied electric field.

According to Equation (2.1), the DEP force depends on the particle size, particle and medium dielectric properties, AC electric field parameters, the interaction between the electric field intensity ($\nabla E_{rms}^{\ 2}$) and the polarization charge, which is closely associated with the polarization factor f_{CM}. The real part of the CM factor (Re[K(ω)]) determines the direction of the DEP force. When Re[K(ω)] is positive (i.e. $\varepsilon_p > \varepsilon_m$), pDEP force will be induced and particles are attracted toward the electric field intensity maxima (Figure 2.1(a)-(c)). On the other head, When Re[$K(\omega)$] is negative (i.e. $\varepsilon_p < \varepsilon_m$), nDEP force will be induced and particles are repelled from the electric field intensity maxima to the minima (Figure 2.1(b)-(d)).

$$\mathrm{Re}\left[\underline{K}(\omega)\right] = \left(\frac{\sigma_p - \sigma_m}{\sigma_p + 2\sigma_m} \right) \quad \text{for} \quad \omega \rightarrow 0 \tag{2.4}$$

$$\mathrm{Re}\left[\underline{K}(\omega)\right] = \left(\frac{\varepsilon_p - \varepsilon_m}{\varepsilon_p + 2\varepsilon_m} \right) \quad \text{for} \quad \omega \gg 0 \tag{2.5}$$

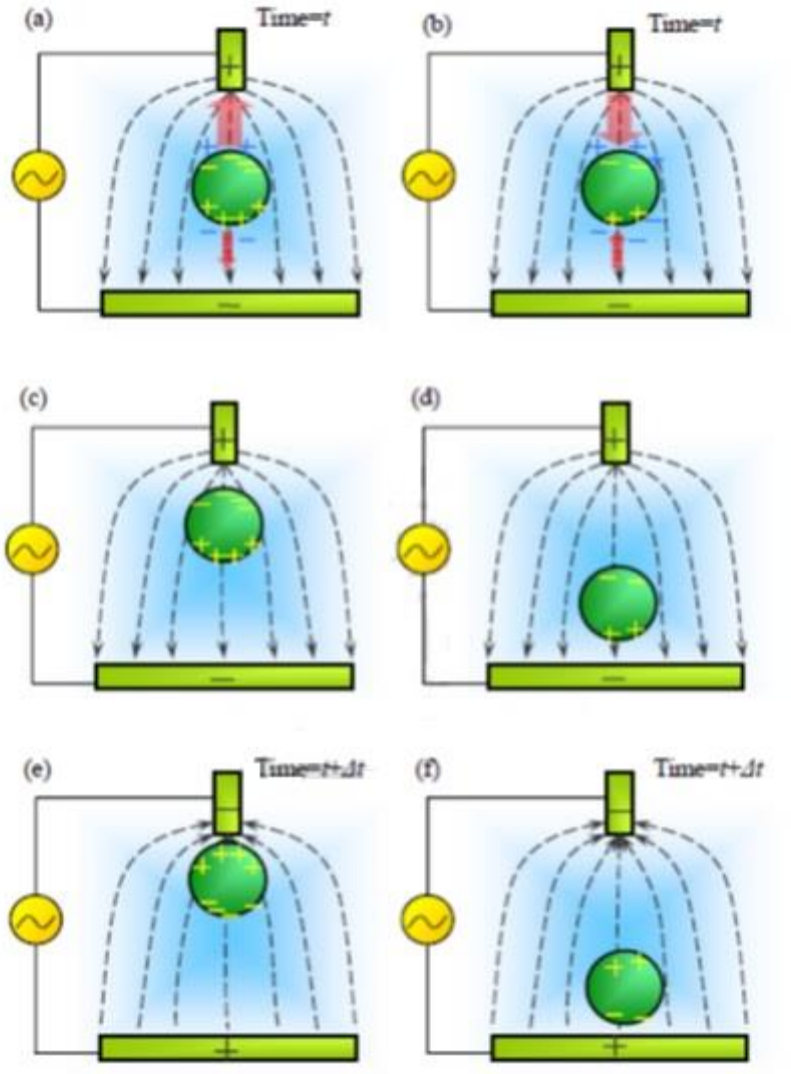

Figure 2.1: A neutral particle of different polarizabilities under the AC electric field

From Equations (2.2), (2.3), it can be seen that the CM factor varies with the applied frequencies. Obviously, DEP forces are strongly frequency driven and controlled. At low frequencies, the conductivity dominates the DEP behavior. On the contrary, the permittivity dominates the DEP behavior at high frequencies (Equations (2.4), (2.5)). When $\sigma_p < \sigma_m$ and $\varepsilon_p > \varepsilon_m$, the particles are under the effect of nDEP at low frequency and under the effect of pDEP at high frequency (Figure 2.2(a)). When $\sigma_p > \sigma_m$ and $\varepsilon_p < \varepsilon_m$, the particles are under the effect of pDEP at low frequencies and under the effect of nDEP at high frequencies (Figure 2.2(b)). When the DEP force changes polarity (from positive to negative or vice versa) and no DEP force acts on a

particle, the frequency applied is defined as the crossing frequency ωc, for which Re[$K(\omega_c)$] = 0.

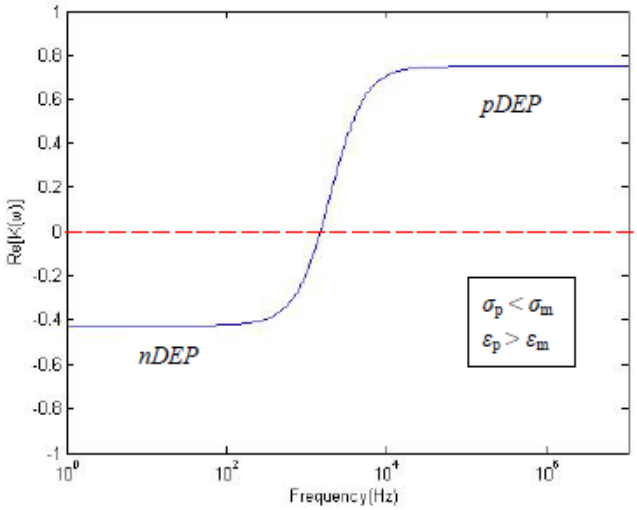

Figure 2.2: (a) for $\sigma_p < \sigma_m$ and $\varepsilon_p > \varepsilon_m$, the particles are under the effect of nDEP at low frequencies and under the effect of pDEP at high frequencies

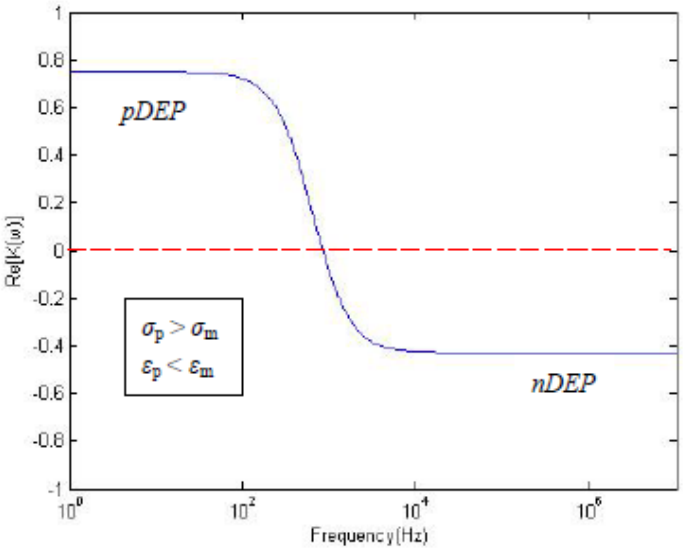

(b) for $\sigma_p > \sigma_m$ and $\varepsilon_p < \varepsilon_m$, the particles are under the effect of pDEP at low frequencies and under the effect of nDEP at high frequencies

2.2 Impedance Measurement

As our purpose is measuring the impedance measurement and one of the most important things which affect it is double layer capacitor so before electrical modeling this term needs to be explained.

2.2.1 Double layer effects

The earliest model of the electrical double layer is usually attributed to Helmholtz. Helmholtz treated the double layer mathematically as a simple capacitor, based on a physical model in which a single layer of ions is adsorbed at the surface. Later Gouy (1909) Chapman (1913) made significant improvements by introducing a diffuse model of the electrical double layer, in which the electric potential decreases exponentially away from the surface to the fluid bulk. The Gouy-Chapman model fails for highly charged double layers. In order to resolve this problem Stern suggested introduction of an additional internal layer, which is now called the Stern layer. The combined Gouy-Chapman-Stern model is most commonly used.

Double layer occur when a metal electrode is immersed into the solution, so the effect of double layer impedance would be considered in this work. When a metal electrode is immersed into the solution, ions in the solution can react with the electrode and the ions from the solution approach the surface of the electrode as closely as possible, and then it leads to complex reactions at the interface. Some of the counter-ions might specifically adsorb near the surface of electrode and build an inner sub-layer, or so-called Stern layer. The outer part of the screening layer is usually called the diffuse layer.

The electric potential on the external boundary of the Stern layer versus the bulk electrolyte is referred to as Stern potential. Electric potential difference between the fluid bulk and the surface is called the electric surface potential. The diffuse layer, or at least part of it, can move under the influence of tangential stress. There is a conventionally introduced slipping plane that separates mobile fluid from fluid that

remains attached to the surface. Electric potential at this plane is called electrokinetic potential or zeta potential. It is also denoted as ζ-potential.

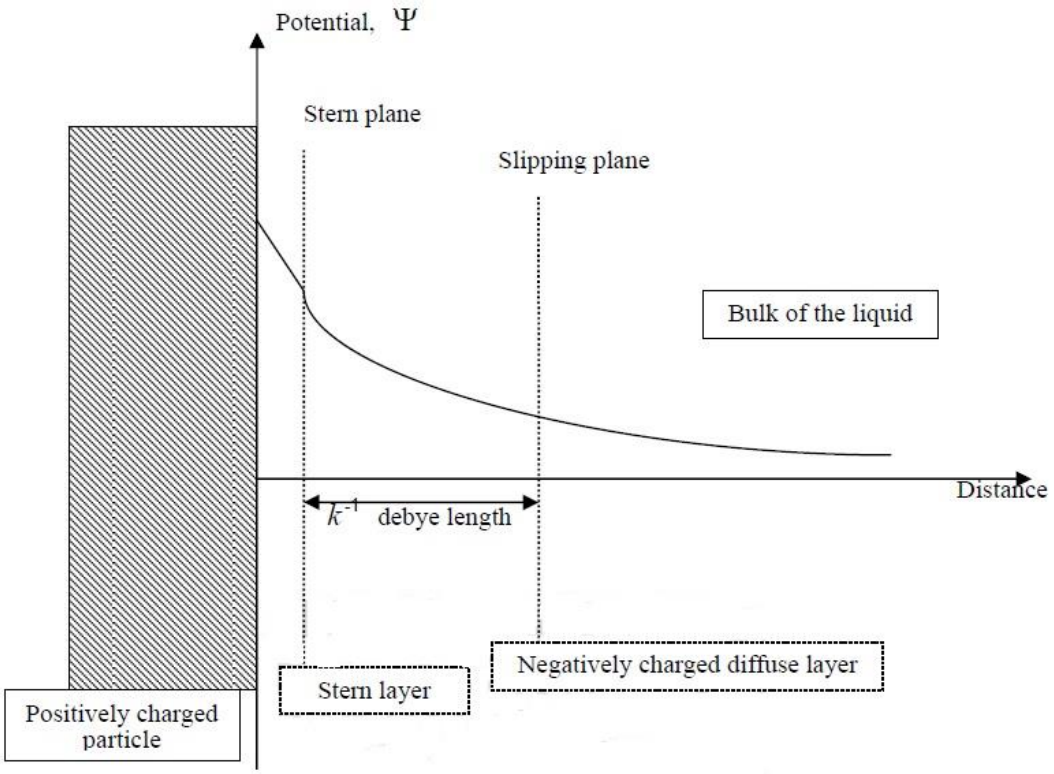

Figure 2.3: Detailed illustration of interfacial Double Layer

Double layer length is known as Debye length (k^{-1}) relates with the ionic type of solution and cellular concentration.

$$k^{-1} = \left(\frac{\varepsilon \varepsilon_0 k_B T}{z^2 C} \right)^{1/2} \tag{2.6}$$

where z denotes the valence of ion and C is the concentration of ions in the electrolyte solution, m^{-3}, T is the absolute temperature in kelvin, k_B is the Boltzmann constant, ε is relative electric permittivity of the medium, and is electric constant. An increase in the permittivity of the medium cause a decrease in the thickness of the double layer at the same time. Decreasing Debye length and raising concentration of ions in solution resulted in an increase in the values of the double layer capacitor.

2.2.2 Electrical modeling

For single cell analysis, cell impedance analysis has developed rapidly and has become an effective method of biological measurement. The electrical parameters of cells are investigated by simulating and can be regarded as an index.

Jang and Wang (2007) proposed a microfluidic device to capture physically single cells and performed impedance measurements at various operational voltage. An equivalent circuit model of the device is established and fits closely to the experimental results. The circuit can be modeled electrically as cell impedance Z_{cell} in parallel with a dielectric capacitance C_{di} and both in series with a pair of electrodes resistor Re, Z_{cell} comprises both cell membrane C_c and cytoplasm R_e. Figure 2.4 schematically depicts the device and the complete process of cell-trapping. Figure 2.5 the equivalent circuit model of the system.

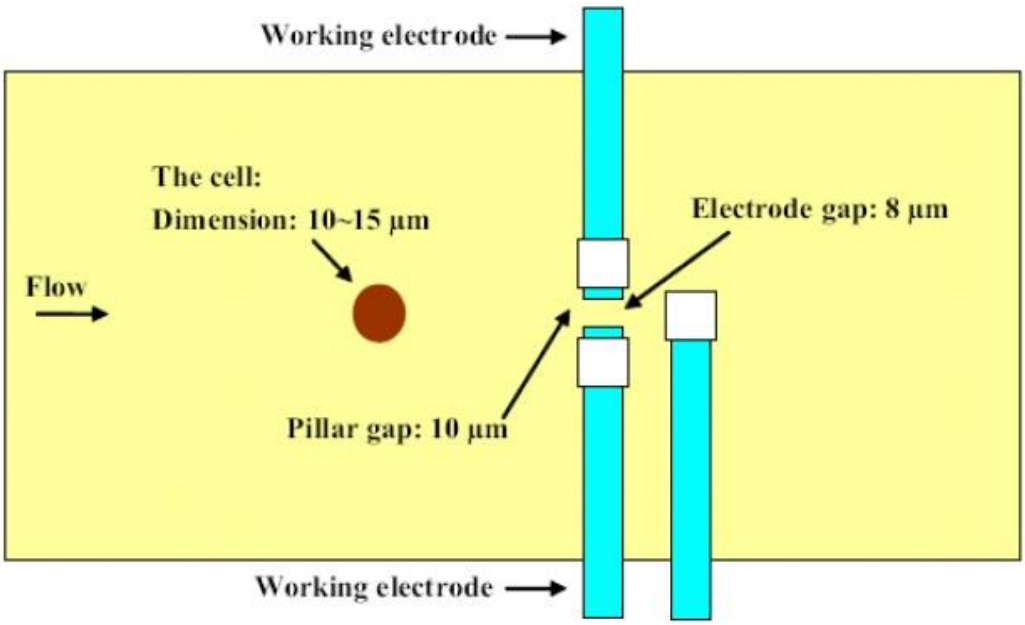

Figure 2.4: Schematically depicts the device and the complete process of cell-trapping

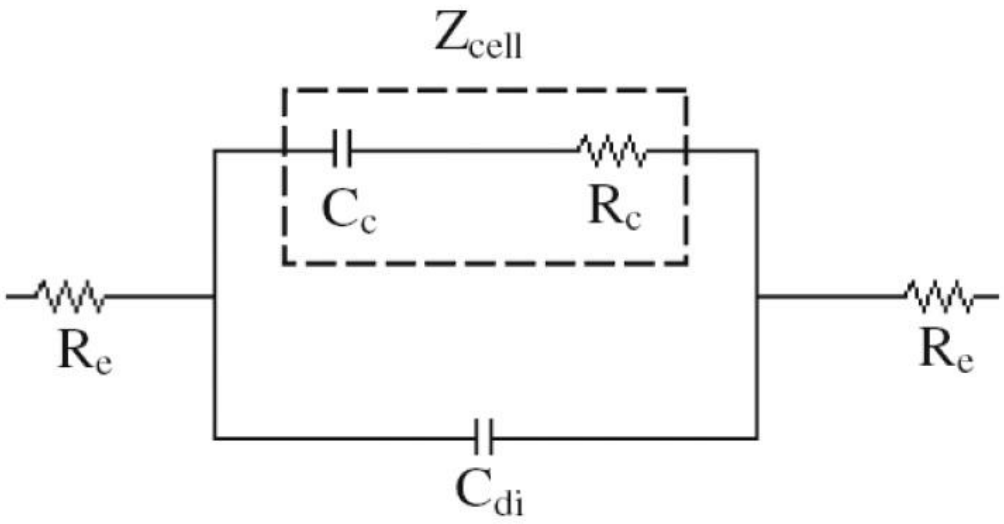

Figure 2.5: The equivalent circuit model of the system

Sun et al. (2008) developed a microfluidic cytometer and describes the analytical and numerical modeling methods for EIS of single cell analysis. Cells pass sequentially through the microfluidic channel at high speed and are analyzed individually. In this circuit model, the impedance of the medium is represented by a resistor and capacitor in parallel. For a viable cell, the membrane has a very low conductivity and can be modeled as a capacitor. At low frequencies, this prevents current flowing through the cell. The cell cytoplasm is represented by a resistor and the capacitance can be ignored to a first approximation. Additionally, the electrode–electrolyte interface impedance is modeled as a capacitor. Figure 2.6 shows schematic of the microfluidic cytometer used for single cell electrical impedance spectroscopy (EIS). As a particle passes through the channel, the measurement is performed using a differential scheme. The two sensing volumes are positioned by the two pairs of parallel facing electrodes. Figure 2.7 a diagram showing the equivalent circuit model for a single cell in suspension. R_m and C_m are the equivalent resistance and capacitance of the medium, respectively. C_{mem} is the equivalent capacitance of the cell membrane. R_i is equivalent resistance of the cell cytoplasm. C_{DL} is the electrical double layer capacitance.

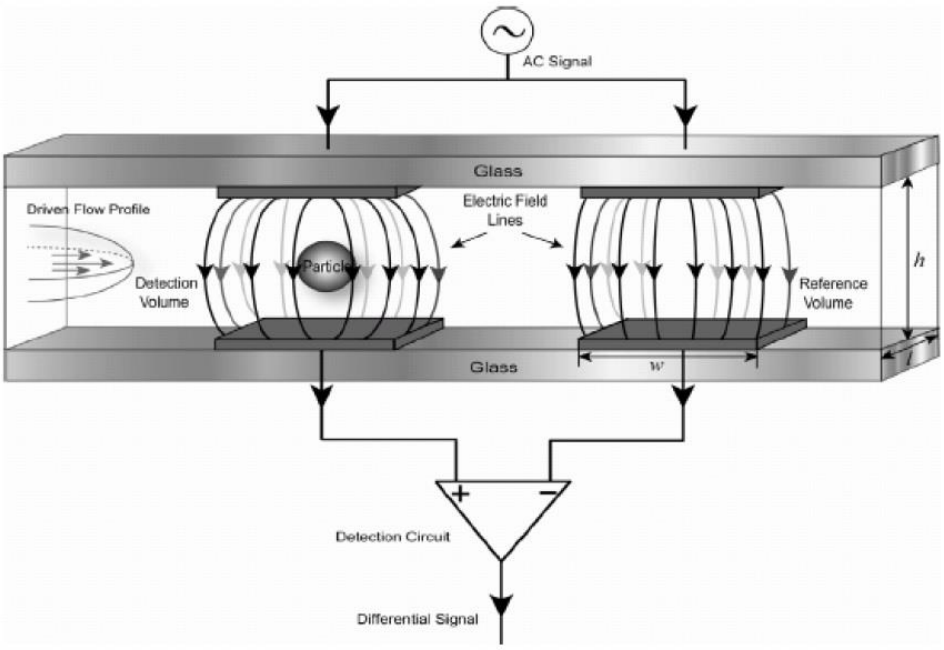

Figure 2.6: Schematic of the microfluidic cytometer used for single cell electrical impedance spectroscopy (EIS). As a particle passes through the channel, the measurement is performed using a differential scheme

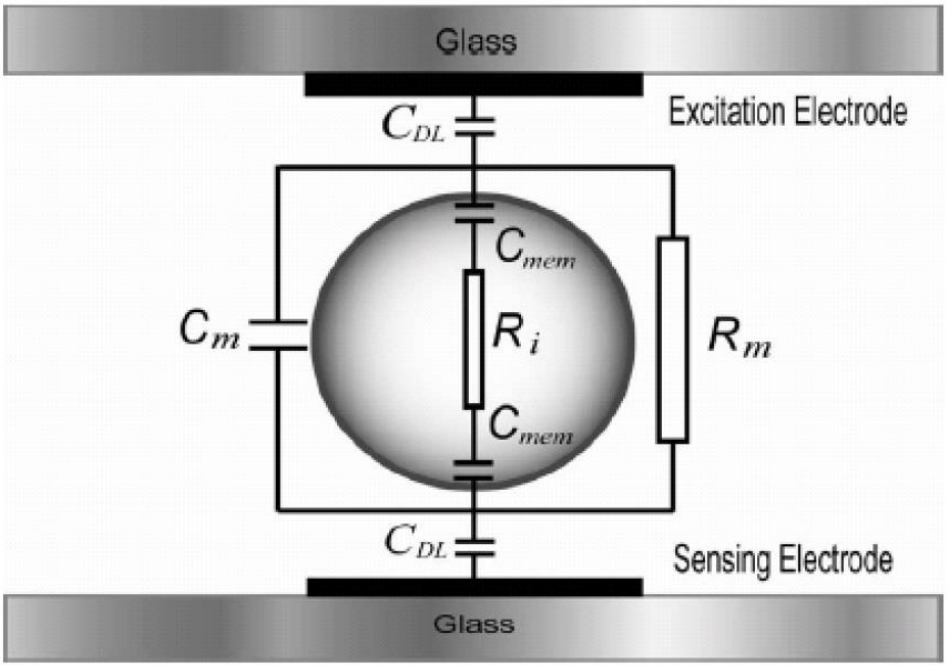

Figure 2.7: A diagram showing the equivalent circuit model for a single cell in suspension

Morgan et al. (2005) developed a device that can simultaneously measure the optical and electrical properties of single cells or other micronscale particles. The micro flow-cytometer chip consists of a planar electrode array onto which a micro-fluidic channel is fabricated from polyimide. The electrodes are used to measure the impedance of single cells flowing through the channel at hundreds per second. A simplified circuit diagram showing a cell between two electrodes is shown in figure 2.8. The circuit comprises a capacitor C_m and resistor R_c representing the cell membrane and the cytoplasm respectively as shown in the figure. This circuit approximates the behavior of a cell in an electric field, where at low frequencies the current flows around the cell and in the limit of high frequencies the current flows without restriction through cell.

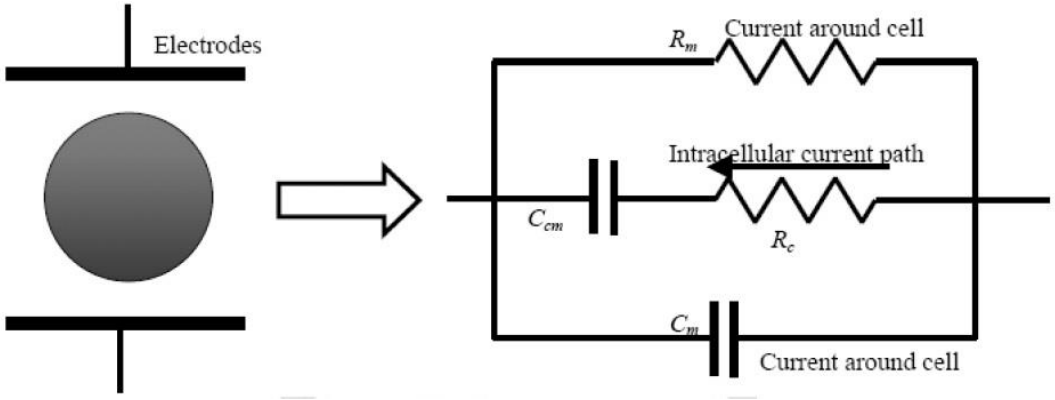

Figure 2.8: Schematic diagram of a cell suspended in an aqueous medium between two electrodes with an applied voltage. The equivalent circuit is shown on the right

2.3 Design

2.3.1 Design of the system

Figure 2.9 shows the schematic view and operation principles of the proposed microfluidic chip. The idea was taken from a work done by Park et al in the year 2010. The chip is composed of trapping chambers connected to the main channel, DEP electrodes, and sensing electrodes. First, particles are introduced into inlet and move through main channel. When a particle arrives at 1st Actuation electrodes, it is forced into trapping chamber by negative DEP (a → b →c →d → e). Then, trapping of the particle can be electrically monitored by measuring the impedance change at sensing electrodes after the positioning of the particle between two sensing

electrodes. Next, the DEP on 1st actuation electrodes is turned off when impedance change was monitored at the 1st sensing electrodes. Then the next particle passes the 1st trapping chamber (a →b →f) and captured into the following trapping chambers by the same method. As explained above The DEP force (F_{DEP}) on a spherical particle is given by Eq. (2.1). The Stokes drag force (F_{drag}) acting on the spherical particle is given as:

$$F_{HD} = 6a\pi\eta v \tag{2.7}$$

where ، a is the radius of the particle, η is the viscosity of the fluid, and v is the velocity of the flow. Then, the particle will be deflected by the action of the DEP force as long as

$$F_{DEP} > F_{HD}\sin\theta = 6a\pi\eta v\sin\theta \tag{2.8}$$

where θ is the angle between the direction of liquid flow and the electrodes. Because the planar actuation electrodes are deposited on the bottom surface of the microchannel, the particle experiences both lateral deflection and vertical lifting force as a result of the combination of the negative DEP and hydrodynamic forces. When a particle is pushed to the side of the microchannel and arrives at the end region of the actuation electrodes (position "d" in Fig. 2.9, it is pushed into the trapping chamber by the negative DEP force.

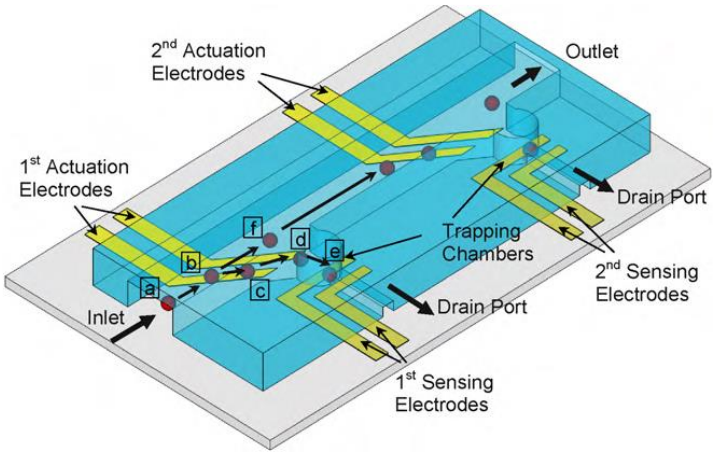

Figure 2.9: Schematic diagram of microfluidic chip Park et al. (2010)

2.3.2 Electrical modeling of the system

The trapping of a particle is monitored by measuring the impedance between the sensing electrodes. The impedance detection is related to the electrode response to the application of a periodic alternating current (AC) signal. Generally, these measurements are carried out at different frequencies. Impedance detection that uses sensing electrodes in an aqueous solution can be modeled as a simple electrical circuit (Fidler and Fernandez, (1989). The impedance without the particle and with a particle can be written as (2.9) and (2.10) respectively. Zhu et al., Without the particle, the impedance between the two electrodes is formed by electrical double-layer capacitance on both electrodes (C_{dl1} and C_{dl2}), resistance of the bulk medium in main channel (R_{e1}) and in drain channel (R_{e2}), and resistance for the trapping zone medium (R_{ts}). After trapping a single particle resistance of the particle (R_{ptc}) which is parellal with resistance of trapping zone will be added to the circuit. Figure 2.10 shows the electrical circuit for both case.

$$Z_{empty} = R_{e1} + R_{e2} + \frac{1}{j\omega C_{dl1}} + \frac{1}{j\omega C_{dl2}} + R_{ts} \tag{2.9}$$

$$Z_{particle} = R_{e1} + R_{e2} + \frac{1}{j\omega C_{dl1}} + \frac{1}{j\omega C_{dl2}} + R_{ts} \tag{2.10}$$

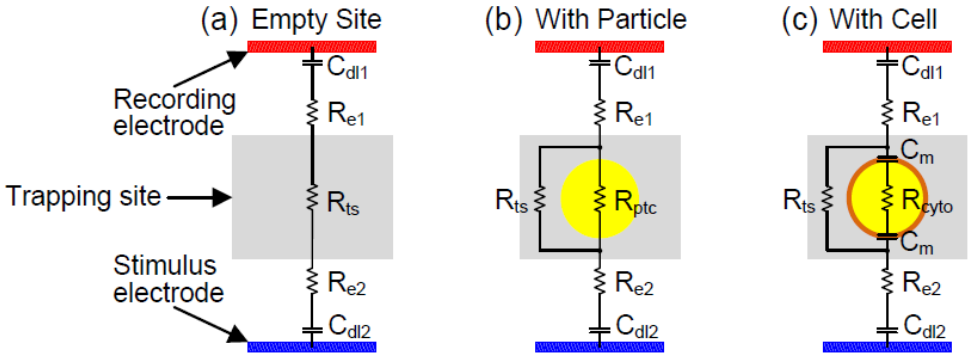

Figure 2.10: Electrical equivalent models without of (a) empty cell trapping site, (b) a site with an immobilized particle, (c) a site with an immobilized cell, Zhu et al. (2008)

3. FABRICATION AND EXPERIMENTAL SETUP

3.1 Chip Fabrication

The microchip is fabricated by MEMS technology using a polydimethylsiloxane (PDMS) layer and a glass substrate that were bonded together.

3.1.1 Mask design

The electrode structures were designed using the Tanner EDA L-edit (v13) layout editor software, saved in GDSII file format, converted to job file and finally transferred to laser writer (DWL 66fs) for writing the mask. The figure 3.1 shows the mask for this study.

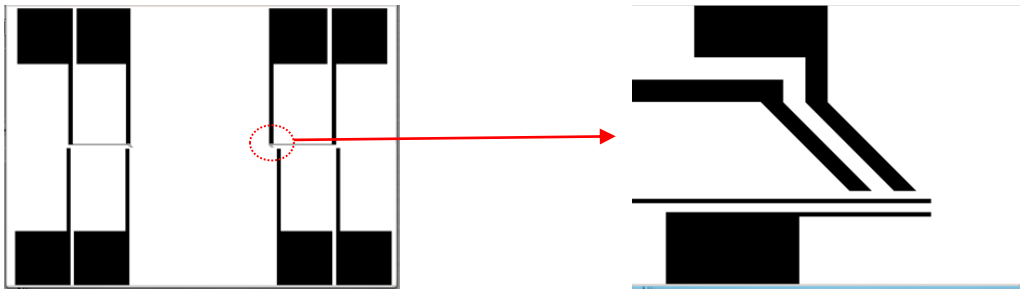

a b

Figure 3.1: a) completed mask b) magnified view of electrodes

3.1.2 Fabrication of glass pattern

Fabrication of glass pattern included deposition of electrodes using electron-beam deposition of titanium which the thickness is about 200 nm. The standard photolithograpy technology and lift off process are used to obtain the electrodes on the glass pattern.

3.1.2.1 Photolithography

Photolithography, also termed optical lithography or UV lithography, is a process used in microfabrication to pattern a substrate. It uses light to transfer a geometric pattern from a photomask to a light-sensitive chemical "photoresist", or simply "resist," on the substrate. A photoresist is a light-sensitive material used in lithography to form a patterned coating on a surface. If a photoresist is positive, mask image is the same as the pattern on the substrate, exposed resist softens and becomes soluble and developer removes the exposed resist to form desired patterns on the substrate. In case of negative photoresist, the patterns on the substrate is the opposite of the mask image, exposed resist hardens and becomes insoluble. Developer removes the unexposed resist from the substrate. The both are shown in figure 3.2. The photolithographic technology processes used to define the pattern of electrode layout and are described as below.

Step 1) microscopic glass (60 × 25 mm) used as substrates. Step 2) Substrates were cleaned in ultrasonic cleaner using 1 molar KOH (potassium hydroxide) for 10 minutes and acetone for another 10 minutes and sequentially rinsed using isopropyl alcohol and DI water to move organic contaminants (such as dust particles or grease) from the glass surface. Finally they're blown dry with nitrogen. Step3) the AZ 1505 positive photoresist was pipette on top and suggested to be spun at 2000 rpm for 30 seconds with Laurell WS-400E spin coating device and final thickness of resist adjusted to be 400 nm on substrates. After spinning, a soft bake was done at 100°C for 50 seconds. Step 4) the next step was to project the image from the mask onto the photoresist .A "OAI Model 200 Mask Aligner" was used to achieve the contact alignment of the photoresist mask. The resist was then exposed to UV light for 5 seconds total. Step 5) the next step was to develop the resist, which was done by placing the substrates in AZ 716 Developer followed by a rinse step in deionized

water. Then baked at 110°C for 50 seconds. Only the areas of resist, which were unexposed to UV light remained.

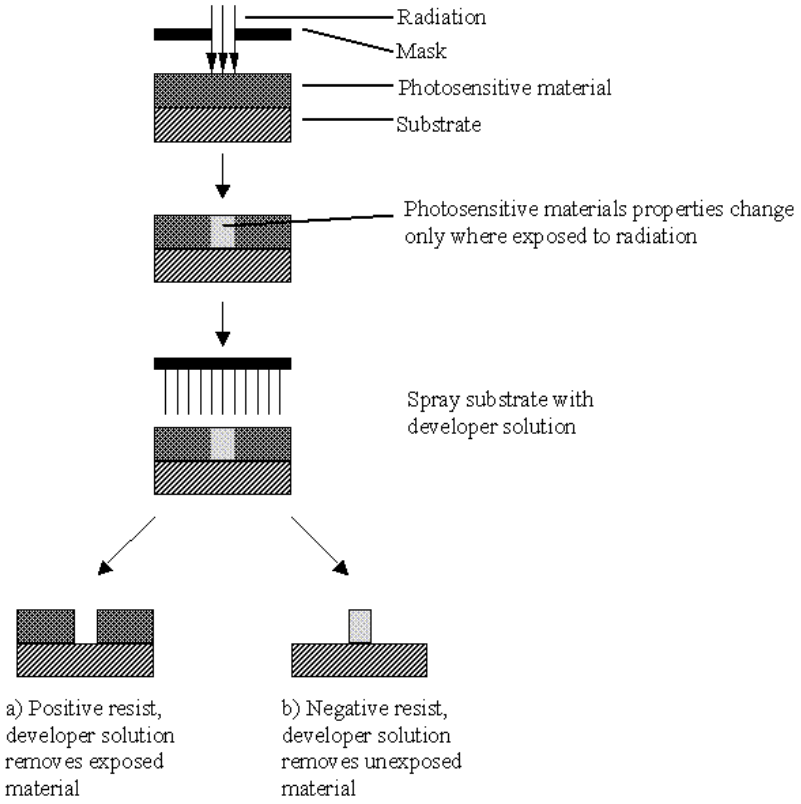

Figure 3.2: Negative and positive photoresist

3.1.2.2 Lift off process

In lift-off processes a sacrificial material, such as photoresist, is first deposited and patterned on the substrate. The material of interest is then deposited on top and the sacrificial material is subsequently removed, leaving behind only the material deposited directly on the substrate.

The metal layers were to be deposited using the electron beam physical vapor deposition (EBPVD) module of "Oncel Advanced Materials and Surface Technologies",(Turkey) Multi-PVD device. Ti target anode is bombarded with an electron beam given off by a charged tunsgten filament under high vacuum at a pressure of at least 7.5 x 10−5 Torr.

The electron beam directed by the magnetic field on to the target anode and causes atoms from the target to vaporize which then precipitate into solid form, coating substrate surface with a thin layer of the anode material. The schematic of an EBPVD system is shown in Fig 3.3.

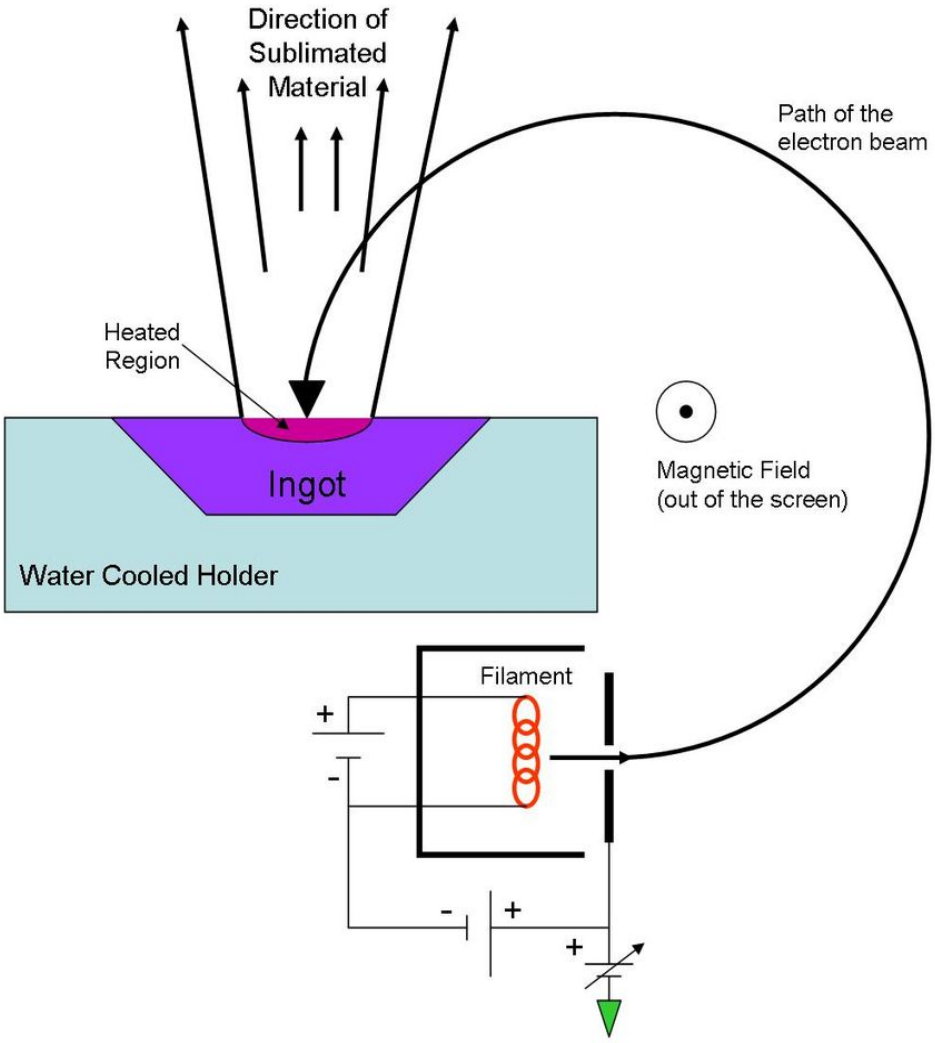

Figure 3.3: The schematic of an EBPVD system

After a 200 nm thickness of Ti deposited on the resist coated and patterned substrate, the remaining resist structures stripped by placing the glass substrates in acetone into a 75-80°C ultrasonic bath for 5-10 minutes. Once dried, the glass wafer was left with only a thin film of electrodes in the shape of the photomask pattern. The fabrication process of glass pattern is shown in figure 3.4. The width of the each pair of electrodes and distance between them were 50µm.

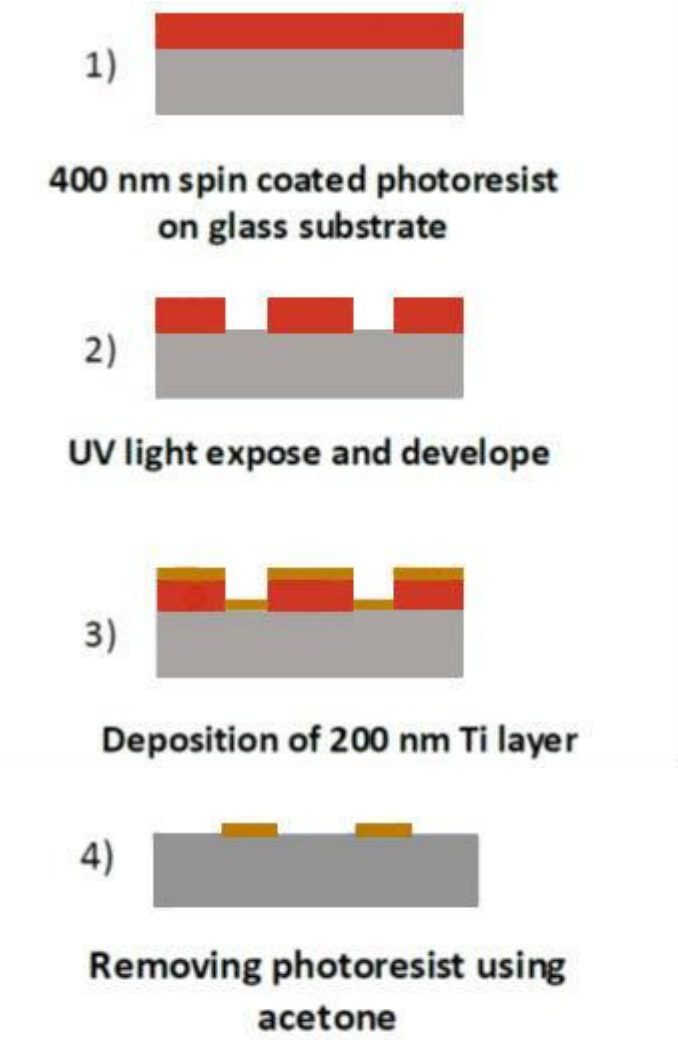

Figure 3.4: Fabrication process for glass pattern

3.1.3 PDMS

Channel structure designed by tanner le edit 13 and mask was written by laser writer as it shown in Figure 3.5.

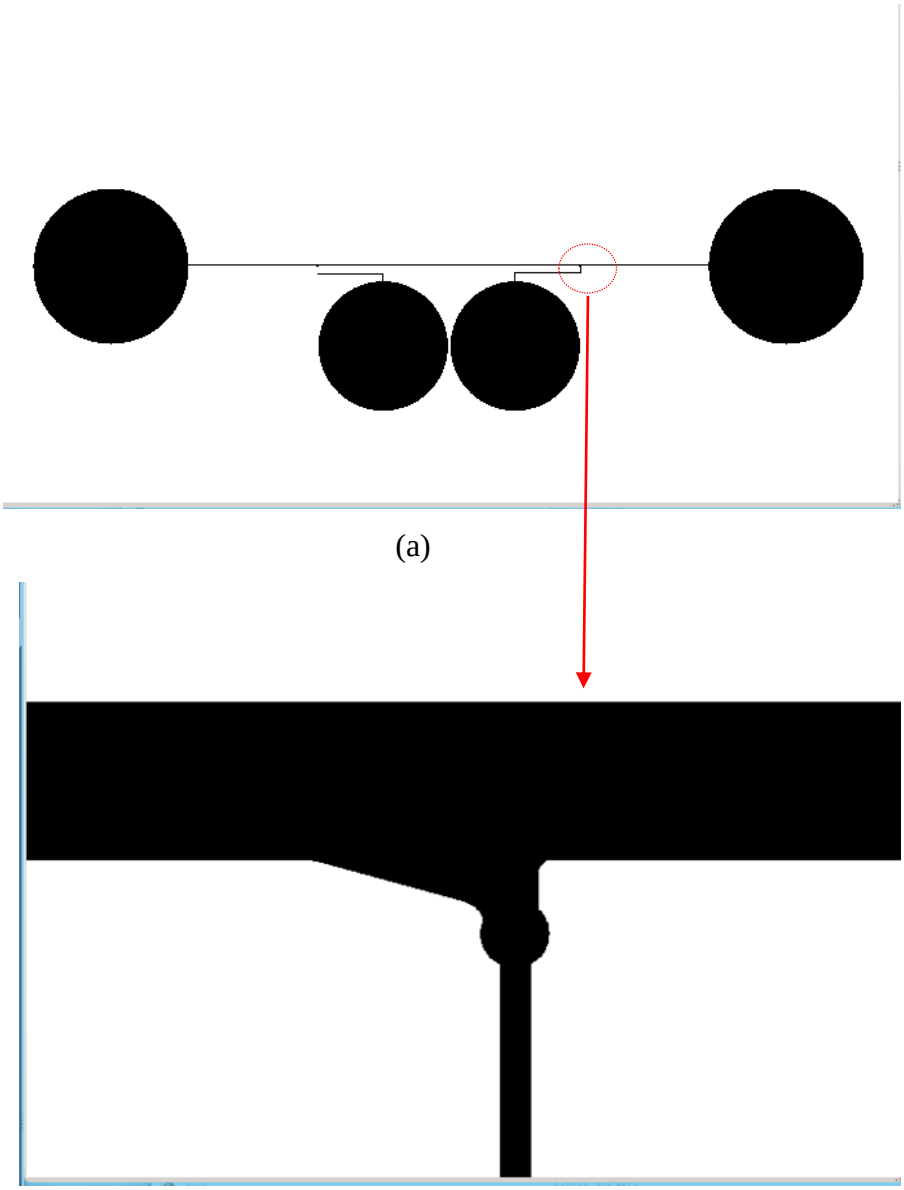

(a)

(b)

Figure 3.5: (a) completed written mask for channel (b) magnified view

A Poly-di-methyl-siloxane (PDMS) chip was created using photolithography. First SU-8 2050 (thickness: 50µm) was applied, followed by UV exposure, to define the channel region. Then, an unexposed region of SU-8 was developed in a commercial SU-8 developer (Microchem Co.) for 6 min. Then, a PDMS was poured onto the mold structure and inherent bubbles were removed in vacuum chamber. Finally, the PDMS was cured at 90 ºC for 15 min and peeled off from the substrate mold. The fabrication process for microchannel is shown in figure 3.6. The access holes for the sample inlet, outlet, and drain port were formed by manual punching. Finally the completed PDMS structure was bonded with the glass substrate after surface treatment by using oxygen plasma cleaner for 1 minutes at a medium level of RF power in a plasma exposure apparatus as shown in figure 3.7.

The width and height of the main channel were 200 and 50µm, respectively. The drain channel was located at the bottom of the trapping chamber, which had dimension of 9 µm width and 50 µm height. The actuation electrodes were placed at the entrance of the trapping chamber to guide the particle into the chamber. For sensing electrodes, one electrode was placed in the trapping chamber and the other in the drain channel to maximize the impedance change when a particle was positioned between these electrodes.

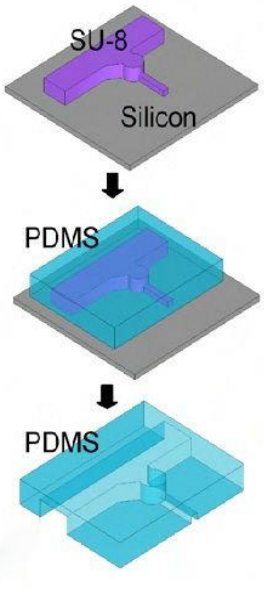

Figure 3.6: Fabrication process for microchannel

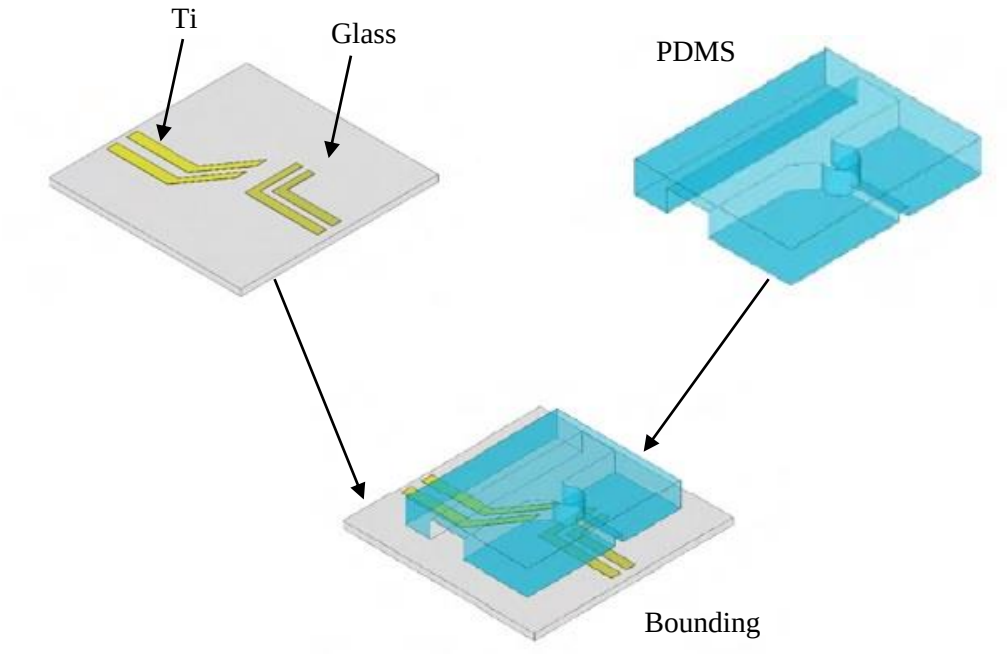

Figure 3.7: Completed structure of the electrodes and channel bonding together

3.2 Experimental Setup

Before experiment the chip needs to be wired which was done by attaching the wires to electrode pads with a silver conductive epoxy due to its good thermal and electrical conductivity. The completed chip shown in figure 3.8 was placed in a microscope setup (Olympus BX51). The applied voltage is produced by function generator (Agilent 81150a). The flow velocity was 1666 µm/s and the voltage applied on the actuation electrodes was set to 10Vpp at 10MHz to apply enough force to trap a particle. Particles manipulation was performed under the microscope. The images of the processes of particle manipulation were acquired by a digital video camera (Olympus DP72).

Impedance spectra was performed using the impedance analyzer (Agilent). The impedance analyzer was calibrated, using short and open standard calibration, before the particle were measured. After a 9.9 µm polystyrene particle was positioned in the trap, the impedance measurements of the trapped single particles were taken at operating voltage of 0.1V- 2 V and frequency range from 3 kHz to 500 kHz. In order to avoid harming the impedance analyzer when the voltage is applied to the trapping structure, a relay should be set between the actuation electrodes and impedance

analyzer and prevents current from flowing through the analyzer directly. The Experimental setup of single particle measurement system is shown in Figure 3.9.

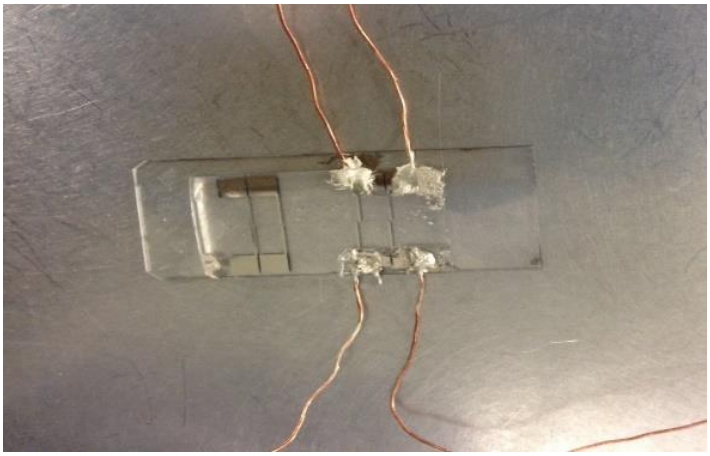

Figure 3.8: Completed chip

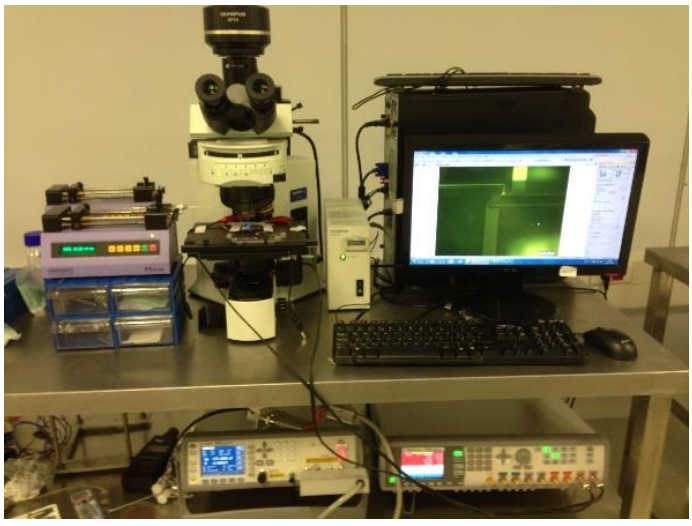

Figure 3.9: Experimental setup

4. RESULTS

4.1 First Generation

Before the new design, another microfluidic design was fabricated with MEMS technology for the purpose of single cell capture and impedance analyzing. It was consisted of two kinds of microelectrodes which are combined to achieve single particle manipulation and trapping. The outer quadrupole electrode is mainly used to manipulate the motion of particles, and the inner microwell, which is composed of one square electrode and another line electrode, is the trap.

After the particle is positioned inside the capture range of the trap, the manipulation electrodes are turned off and the trap electrodes are actuated (Jang et al., 2009). The nDEP microwell demonstrated by Rosenthal & Voldman (2005) at used to achieve single particle trapping. In order to integrate the measurement electrodes into this structure, the square electrode is separated into two parts, which are regarded as the measurement electrodes (Hong et al., 2012).

The inner length of the square electrode was designed to be 25 μm to fit the sizes of particles which is about 9.9 μm and 3.2 μm. Figure 4.1 shows the mask written for this design with DWL 66fs laser writer.

The device utilizes DEP and ACET to capture a single cell and measure its impedance. The quadrupole electrodes are energized to accumulate single cells at the center with ACET. ACET fluid flow arises from the interaction of the external electric field with temperature induced inhomogeneities in medium conductivity and permittivity due to Joule heating. To guide single cells to the microwell, some of the electrodes are turned off while others remain on. When a single cell approaches the microwell, the applied voltage is reduced to prevent the particle from passing through the microwell.

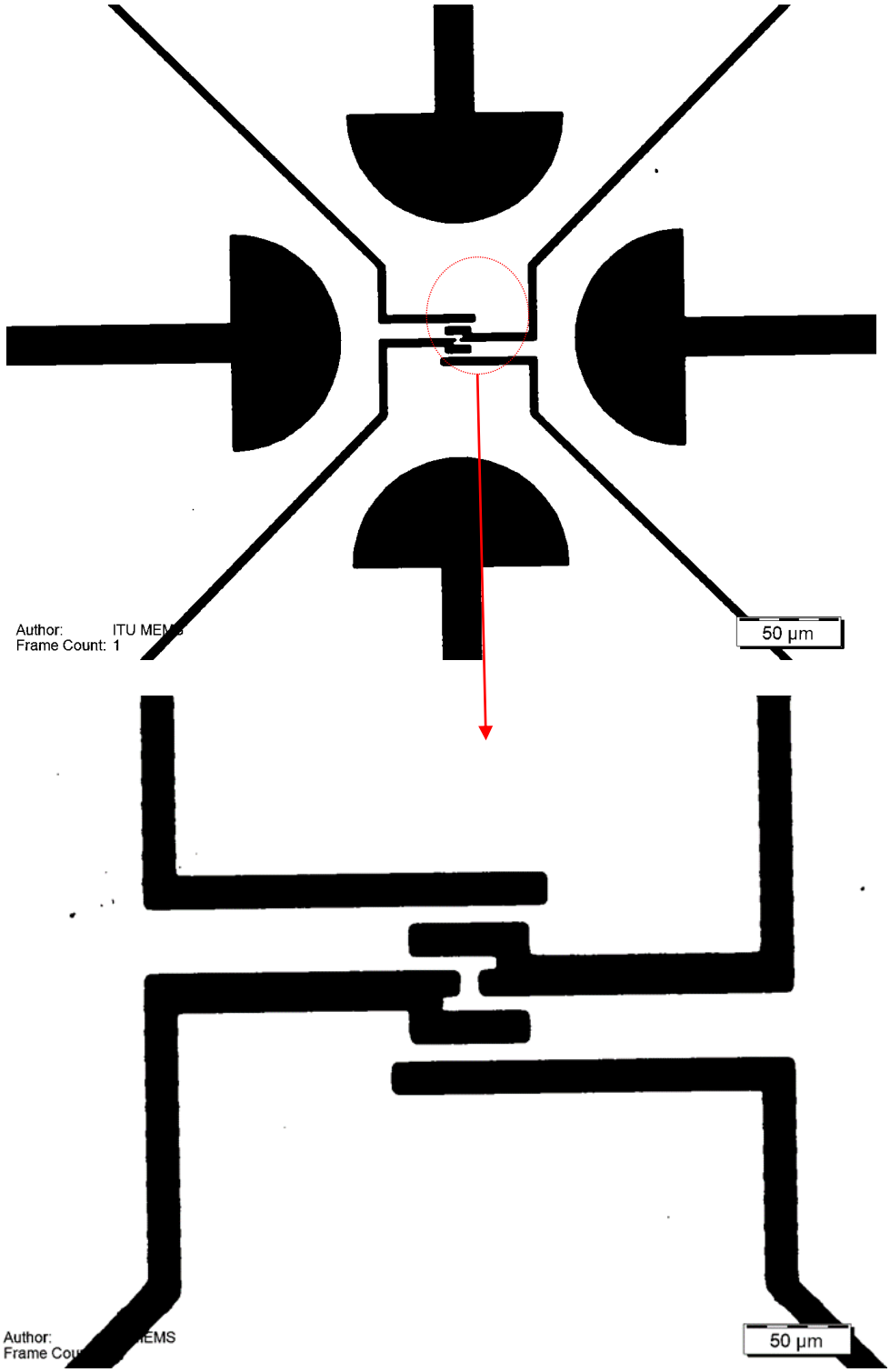

Figure 4.1: a) completed mask b) magnified view

After a single cell is positioned in the trap, the energized electrodes are turned off. Finally, the microwell trap is activated by applying an AC electric field of 5 MHz and 10 Vpp to capture the cells.

Polystyrene particles are trapped by the plane electric microwell and visually inspected using an optical microscope (Olympus BX51) during the experimental process as shown in figure 4.2.

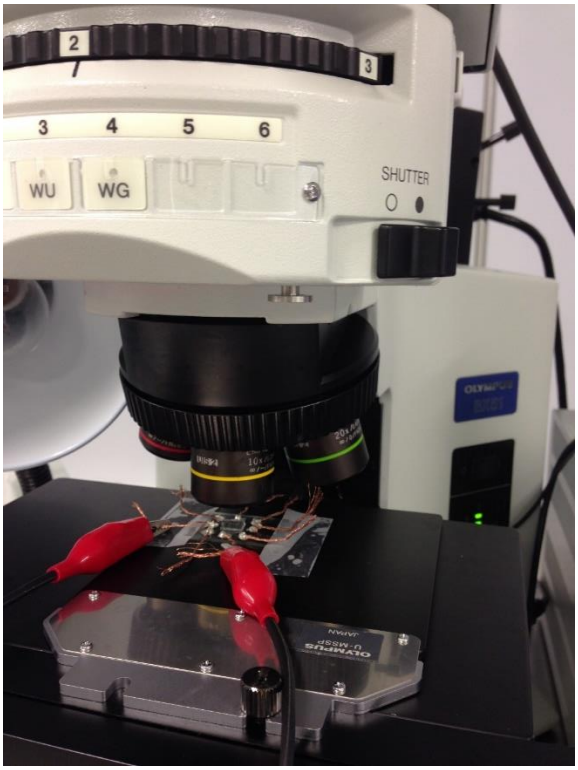

Figure 4.2: Experimental setup for single particle capture

At first, a drop of the medium with suspended particles is dribbled on the PDMS. Medium conductivity was about 1.20 S/m. Then, the voltages of 5Vpp-10Vpp at 5 MHz applied to the quadrupole electrodes in the manipulation process are produced by a function generator (Agilent 81150a). As the recorded images during the experiments are not clear enough. Therefore for understanding the following experiment better, Pixler application used to clarify the electrodes as shown in figure 4.3. Figure 4.4 and 4.5 presents some results of trapping of polystyrene particles with size of 9.9 and 3.2 µm respectively.

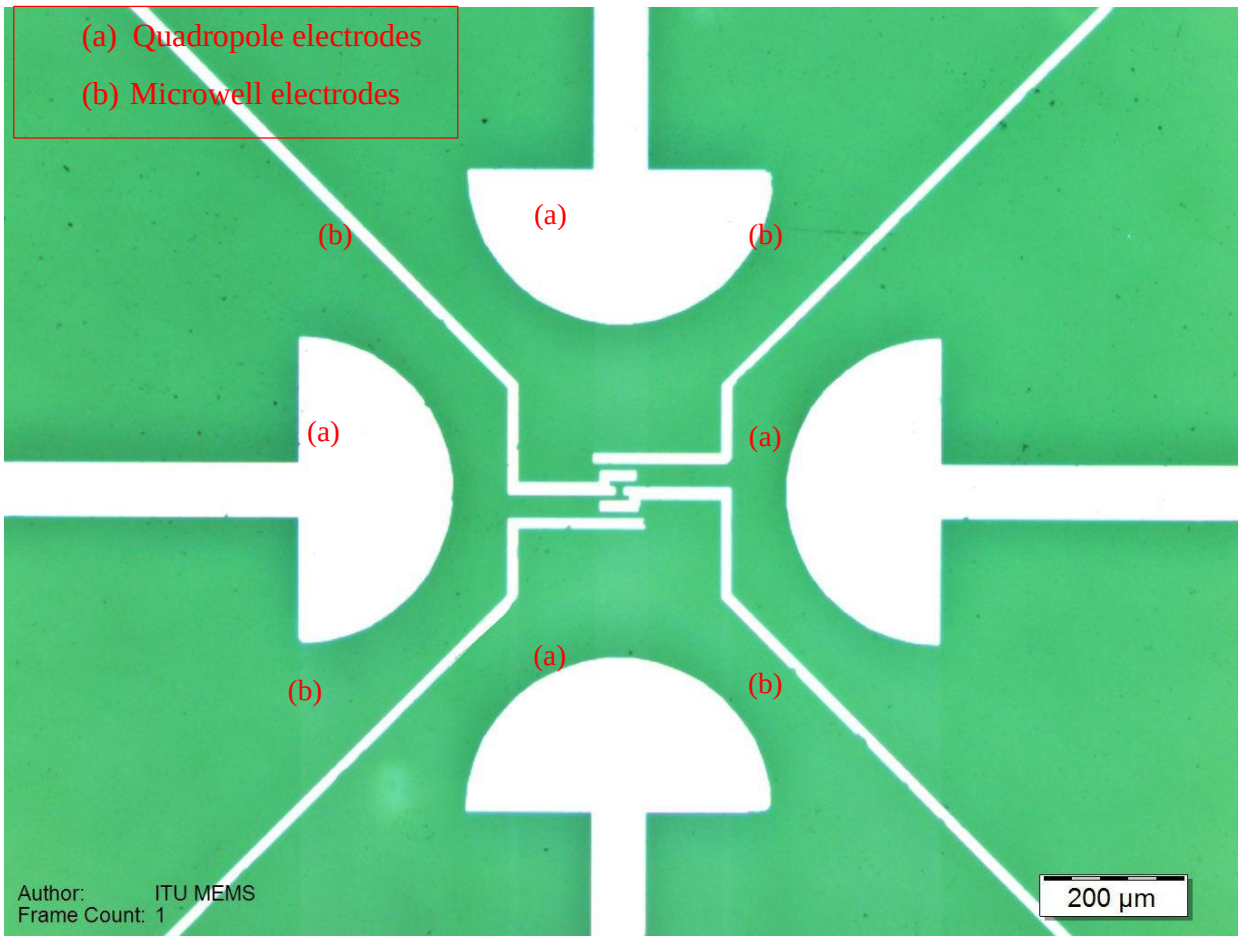

Figure 4.3: Quadropole electrodes (a) and microwell electrodes (b) for capturing a a single particle

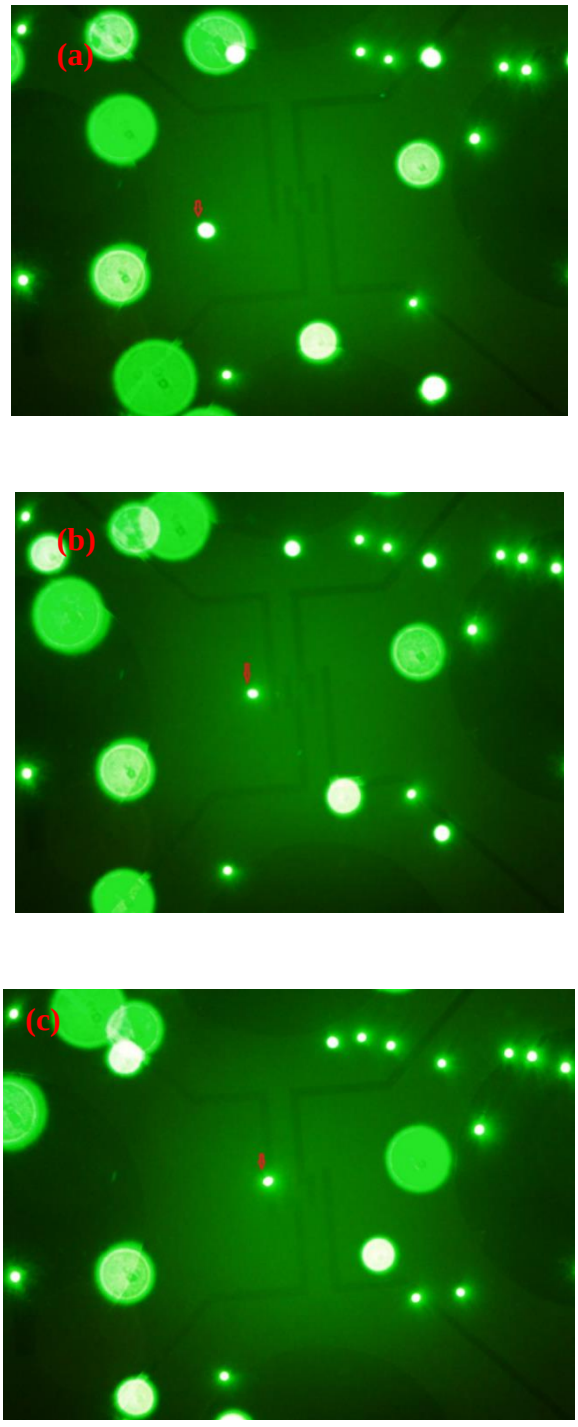

Figure 4.4: a-c) Sequence of directing a 9.9 µm polystyrene particle with quadropole electrodes using ACET at 5 MHz at 10 Vp-p

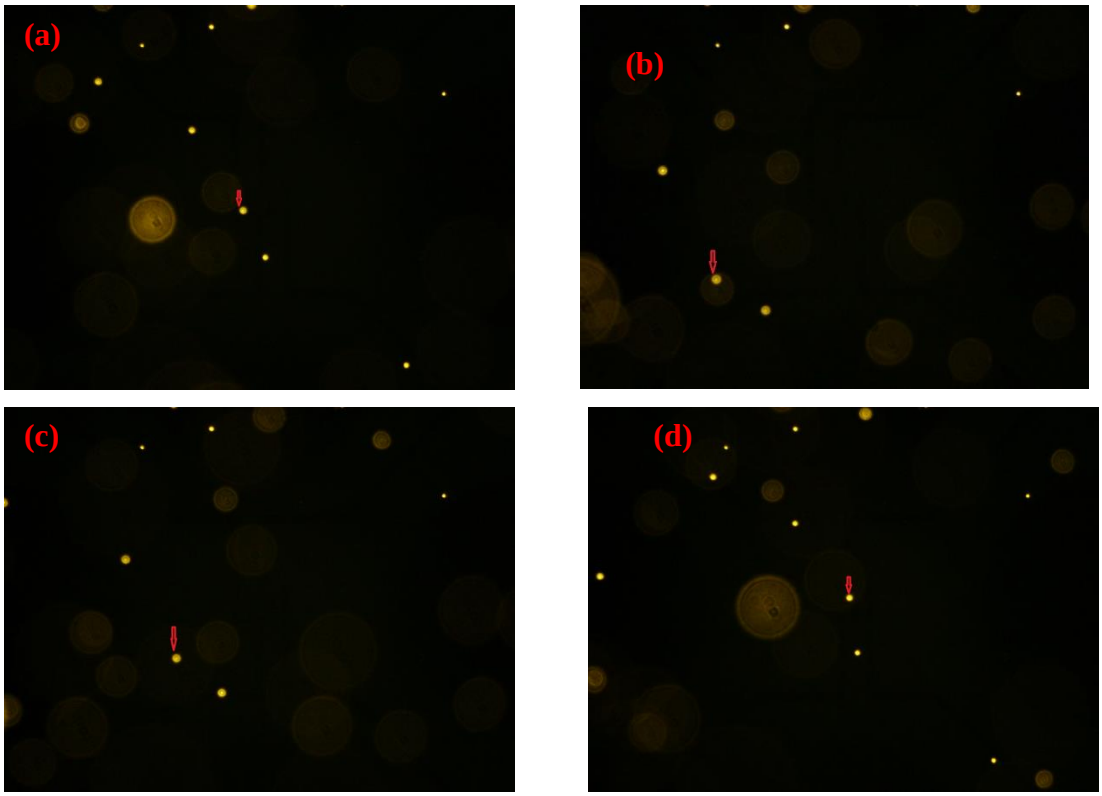

Figure 4.5: a-d) Sequence of directing a 3.2 µm polystyrene particle with quadropole electrodes using ACET at 5 MHz and 10 Vp-p

4.2 New Design

For the purpose of trapping a particle with a more simple design which made both the process of fabrication and experiments easier and faster and gives results in impedance measurement with a higher accuracy, a new design which the theory and design explained deeply in this study decided to be fabricated.

4.3 Single Particle Trapping

In this study, a group of particles and a single one trapped. As the recorded images during the experiments are not clear enough. Therefore for understanding the following experiment better, Pixler application used to clarify the electrodes and microchannel as shown in figure 4.6. Trapping process of a group of particles and a single one done and visually inspected using an optical microscope during the experimental process. The process of trapping for a group of cells and a particle

explained with Figure 4.7 and 4.8 respectively. At first the channel filled with a syringe pump to prevent air trapping during the experiment. The experiments done with two suspending medium, DI water and 150 mM NaCl with conductivities of 0.0001 S/m and 0.001 respectively. Then polystyrene particles with 9.9µm loaded to inlet port. The flow rate was about 10 µl/min until particles coming close to the trapping chamber. Then it reduced to 1 µl/min with velocity of 1666 µm/s to have a strong DEP force which overcomes hydrodynamic friction exerted by the fluid flow and lead particle to the desired direction.

In the case of single particle after capturing, the pump turned off to prevent trapping more particle into the trapping chamber. So in the next step the impedance measured successfully. Both the width of the electrodes and the height of the channel was 50µm. Also the frequency and voltage of applied DEP signal was 10 MHz and 10 Vp-p respectively to apply enough force to trap a particle.

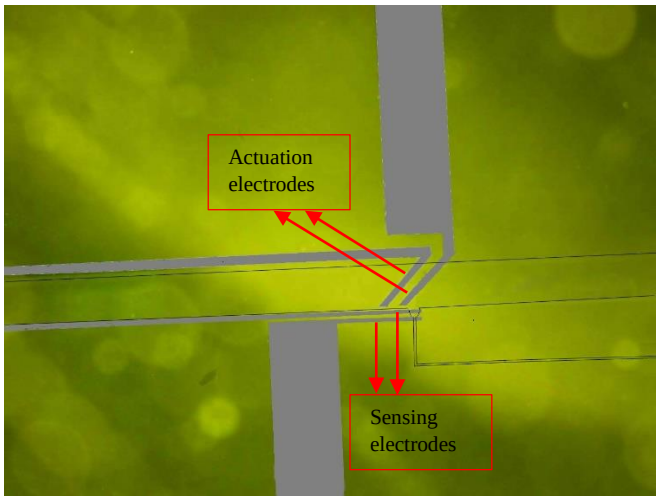

Figure 4.6: Actuation and sensing electrodes used for experiments

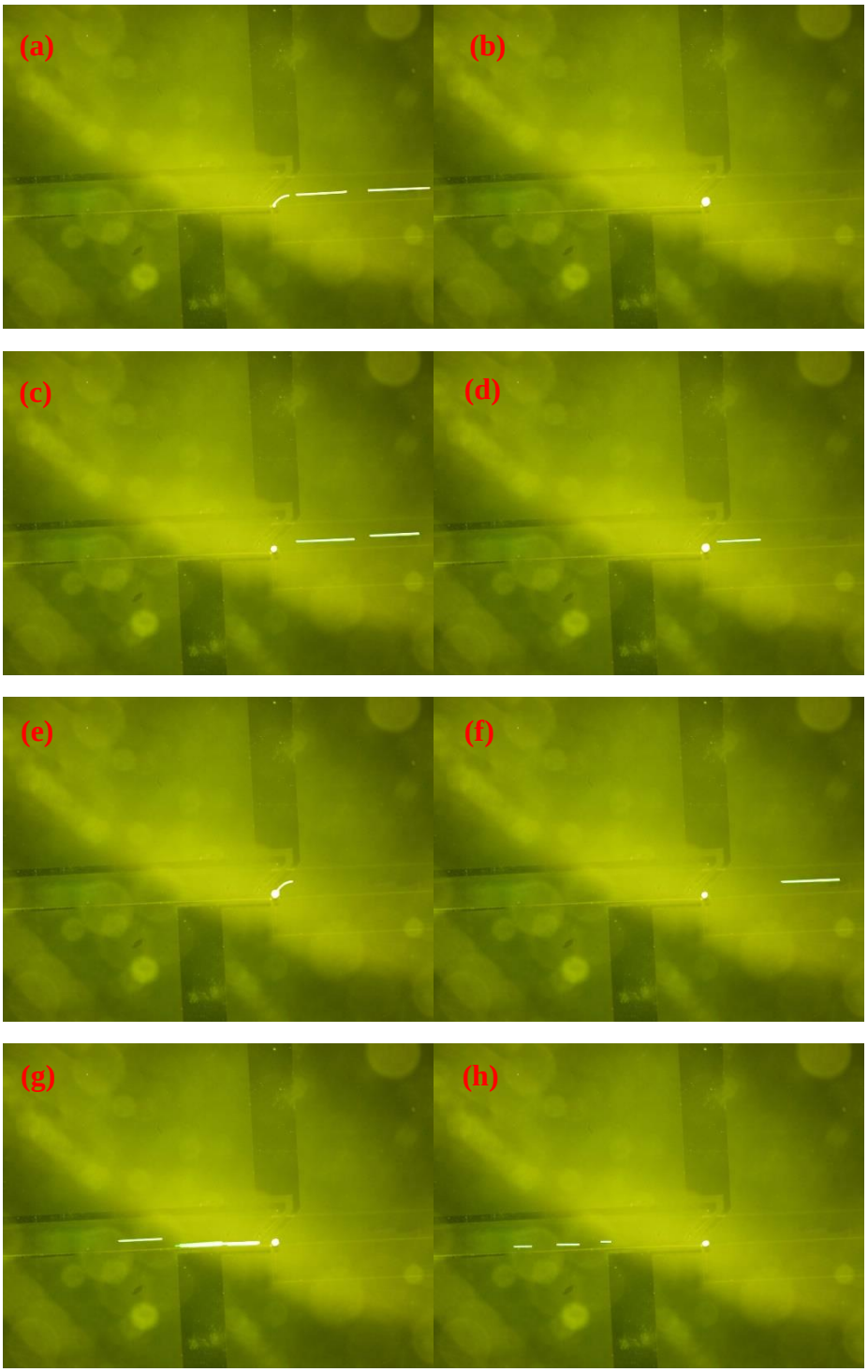

Figure 4.7: a) Particle are flowing with a rate of 1 µl/min coming close to trap. b-f) shows trapping of particles by applying 10 MHz and 10 Vp-p with negative dielectrophoresis. g&h) after turning off the function generator trapped particles started moving again

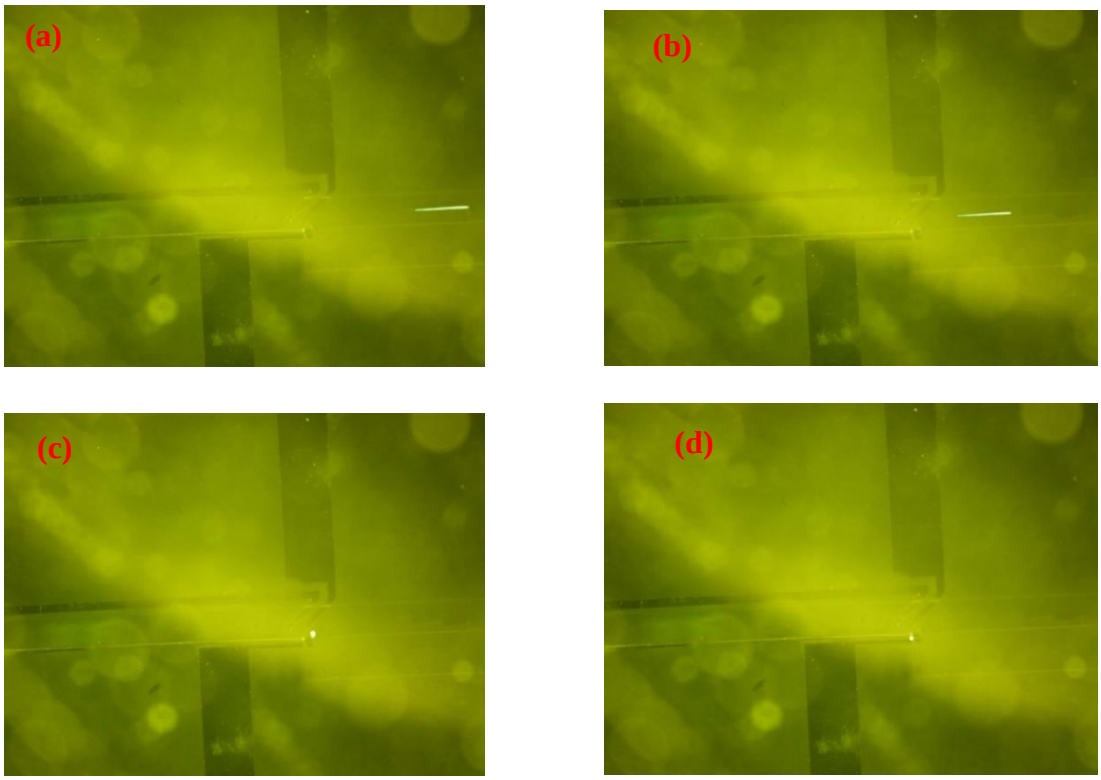

Figure 4.8: a and b) a Particle with a rata of 1 µl/min is coming close to trap. c) Shows trapping of particles by applying 10 MHz and 10 Vp-p d) Turn off the pump to prevent the trapping of more particles so a single particle can be trapped and the impedance or other properties can be measured

4.4 Particle Characteristic Analysis

After a polystyrene particle was exactly positioned between sensing electrodes when the negative DEP prevailed the drag force. Impedance of it measured by an impedance analyzer. The data obtained from the experiment are shown in Tables 4.1- 4.11.

Table 4.1: Results of impedance spectrum in DI water at 0.2 V

Frequency (Hz)	*Z* (without particle) (MΩ)	*Z* (with particle) (MΩ)
3557	66.66 ± 0.97	73.50 ± 0.86
8111	45.59 ± 0.48	49.92 ± 0.52
18490	12.87 ± 0.32	14.39 ± 0.46
42170	6.40 ± 0.13	7.01 ± 0.11
96160	2.75 ± 0.02	3.12 ± 0.09
219300	1.15 ± 0.01	1.24 ± 0.07
500000	0.48 ± 0.02	0.52 ± 0.03

Table 4.2: Results of impedance spectrum in DI water at 0.4 V

Frequency (Hz)	*Z* (without particle) (MΩ)	*Z* (with particle) (MΩ)
3557	78.77 ± 2.14	85.99 ± 1.95
8111	53.52 ± 1.67	57.78 ± 2.01
18490	14.59 ± 0.19	16.13 ± 0.23
42170	7.42 ± 0.14	8.19 ± 0.18
96160	3.57 ± 0.44	4.02 ± 0.36
219300	1.42 ± 0.13	1.59 ± 0.21
500000	0.58 ± 0.05	0.65 ± 0.12

Table 4.3: Results of impedance spectrum in DI water at 0.6 V

Frequency (Hz)	*Z* (without particle) (MΩ)	*Z* (with particle) (MΩ)
3557	60.75	66.31
8111	44.28	48.96
18490	12.60	14.1
42170	6.25	6.78
96160	2.69	2.95
219300	1.13	1.23
500000	0.47	0.51

Table 4.4: Results of impedance spectrum in DI water at 0.8 V

Frequency (Hz)	*Z* (without particle) (MΩ)	*Z* (with particle) (MΩ)
3557	60.75 ± 1.27	61.35 ± 2.31
8111	44.28 ± 0.47	50.23 ± 1.25
18490	12.60 ± 0.25	14.11 ± 0.94
42170	6.25 ± 0.11	7.09 ± 0.58
96160	2.69 ± 0.05	2.96 ± 0.16
219300	1.13 ± 0.02	1.27 ± 0.12
500000	0.47 ± 0.11	0.53 ± 0.9

Table 4.5: Results of impedance spectrum in DI water at 1 V

Frequency (Hz)	*Z* (without particle) (MΩ)	*Z* (with particle) (MΩ)
3557	118.15	130.96
8111	66.11	71.92
18490	25.11	28.16
42170	15.36	17.11
96160	6.21	6.80
219300	2.44	2.67
500000	0.92	1.03

Table 4.6: Results of impedance spectrum in 150mM NaCl at 0.1 V

Frequency (Hz)	*Z* (without particle) (MΩ)	*Z* (with particle) (MΩ)
3557	5.78 ± 0.18	6.36 ± 0.21
8111	2.99 ± 0.03	3.33 ± 0.08
18490	1.54 ± 0.00	1.68 ± 0.02
42170	0.79 ± 0.00	0.88 ± 0.01
96160	0.40 ± 0.00	0.44 ± 0.00
219300	0.20 ± 0.00	0.23 ± 0.00
500000	0.10 ± 0.00	0.12 ± 0.00

Table 4.7: Results of impedance spectrum in 150mM NaCl at 0.2 V

Frequency (Hz)	*Z* (without particle) (MΩ)	*Z* (with particle) (MΩ)
3557	5.78	6.36
8111	3.04	3.34
18490	1.55	1.69
42170	0.80	0.89
96160	0.41	0.45
219300	0.20	0.22
500000	0.10	0.11

Table 4.8: Results of impedance spectrum in 150mM NaCl at 0.4 V

Frequency (Hz)	*Z* (without particle) (MΩ)	*Z* (with particle) (MΩ)
3557	5.54 ± 0.01	6.11 ± 0.04
8111	2.96 ± 0.01	3.17 ± 0.02
18490	1.52 ± 0.00	1.66 ± 0.01
42170	0.79 ± 0.00	0.88 ± 0.00
96160	0.41 ± 0.00	0.44 ± 0.00
219300	0.21 ± 0.00	0.23 ± 0.00
500000	0.10 ± 0.00	0.11 ± 0.00

Table 4.9: Results of impedance spectrum in 150mM NaCl at 0.6 V

Frequency (Hz)	*Z* (without particle) (MΩ)	*Z* (with particle) (MΩ)
3557	5.47 ± 0.02	6.12 ± 0.06
8111	2.94 ± 0.01	3.22 ± 0.04
18490	1.52 ± 0.01	1.68 ± 0.03
42170	0.79 ± 0.00	0.86 ± 0.01
96160	0.41 ± 0.01	0.44 ± 0.00
219300	0.21 ± 0.00	0.23 ± 0.00
500000	0.19 ± 0.00	0.12 ± 0.00

Table 4.10: Results of impedance spectrum in 150mM NaCl at 1 V

Frequency (Hz)	*Z* (without particle) (MΩ)	*Z* (with particle) (MΩ)
3557	5.65	6.22
8111	3.02	3.31
18490	1.54	1.68
42170	0.80	0.89
96160	0.41	0.46
219300	0.21	0.24
500000	0.11	0.12

Table 4.11: Results of impedance spectrum in 150mM NaCl at 2 V

Frequency (Hz)	*Z* (without particle) (MΩ)	*Z* (with particle) (MΩ)
3557	5.30 ± 0.04	5.86 ± 0.08
8111	2.89 ± 0.01	3.18 ± 0.05
18490	1.47 ± 0.00	1.62 ± 0.03
42170	0.76 ± 0.00	0.85 ± 0.01
96160	0.40 ± 0.00	0.44 ± 0.00
219300	0.21 ± 0.00	0.24 ± 0.00
500000	0.11 ± 0.00	0.12 ± 0.00

Figures 4.9- 4.13 shows the impedance spectrums in magnitude of polystyrene particles before and after trapping in DI water and figure 4.14- 4.19 shows the impedance spectrum of particle in 150 mM before and after trapping. The impedance was measured at different voltages ranges (0.1-2 V) between 3 KHz and 500 KHz. The impedance increase can be explained by a gradual blockage of the electrical path between the sensing electrodes. The impedance measurement over wide frequency range revealed that the impedance decreased as the frequency increased because of the double-layer capacitance on each electrode. In addition, the increment ratio was more evident for the particle experiment at the low frequency. Also it is obvious that with increasing the voltage, it was a slight decrease in impedance in most of frequencies. Furthermore comparison of the obtained results for DI water and 150mM NaCl shows less impedance magnitudes for 150mM NaCl which can be described due to increase of the conductivity of the suspending medium. The results of impedance increased for each frequency in different voltages are shown in Tables 4.12 and 4.13 for DI water and Nacl, respectively. Impedance measurements were carried out several times for each voltage in some of experiments. For this reason the range of error are added in some Tables. In Figures 4.20 and 4.21 upper limit, lower limit and mean curves of impedance increased are shown. The mean of impedance increased in DI water is 10.13% and in Nacl is 10.20%. Although different solutions are used for impedance evaluation of polystyrene particles, results in both case are close to each other with approximately 10% increasing. The work of Park et al. (2010) tends to support this assertion which states polystyrene particles increase impedance which is close to 10%.

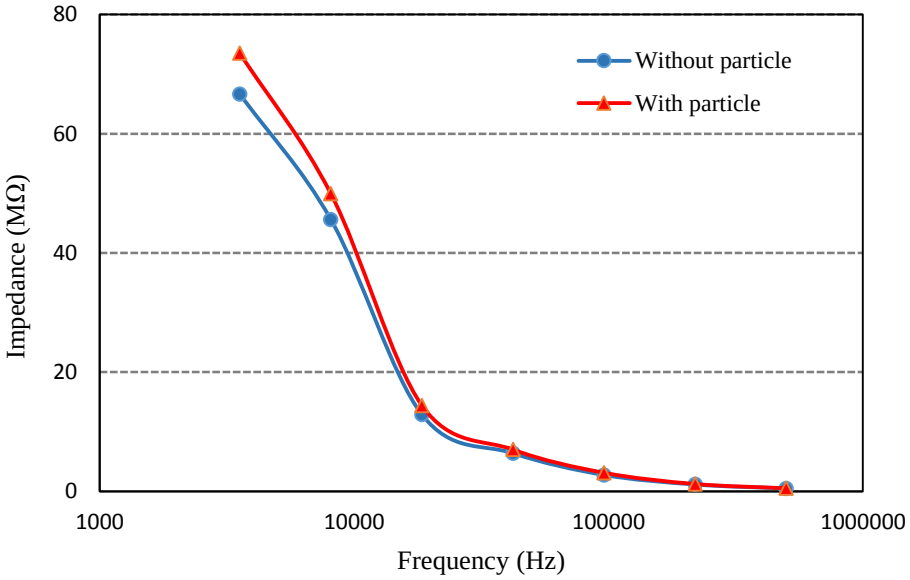

Figure 4.9: Impedance measurement results of polystyrene microparticle experiments in DI water at 0.2 V

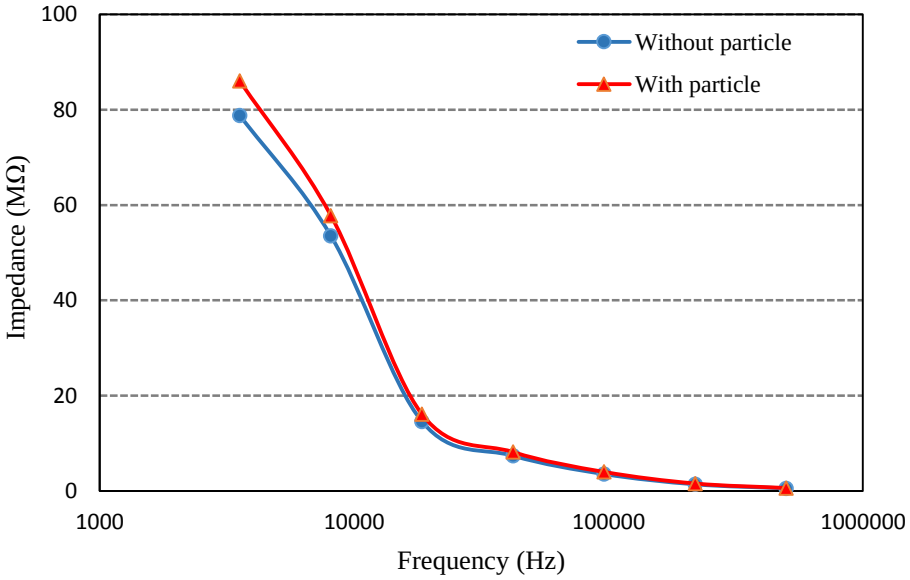

Figure 4.10: Impedance measurement results of polystyrene microparticle experiments in DI water at 0.4 V

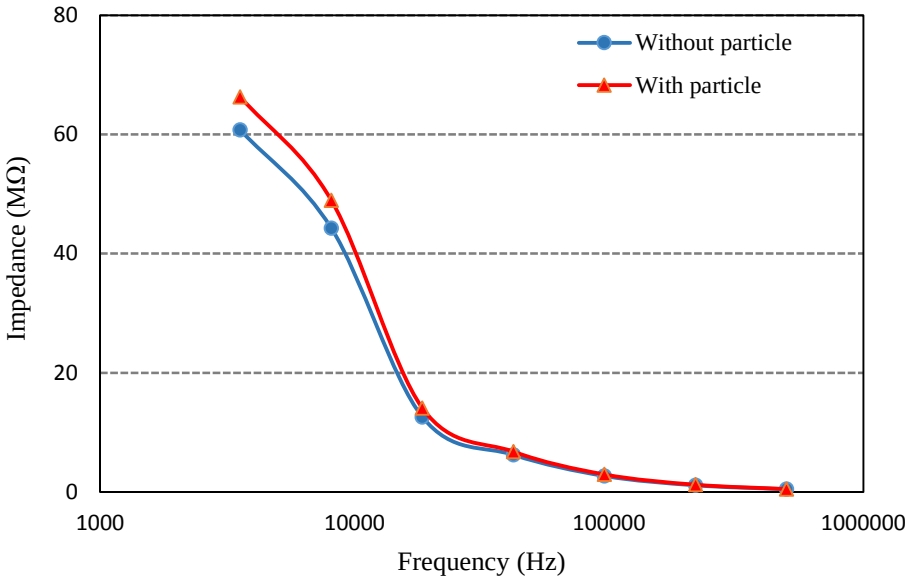

Figure 4.11: Impedance measurement results of polystyrene microparticle experiments in DI water at 0.6 V

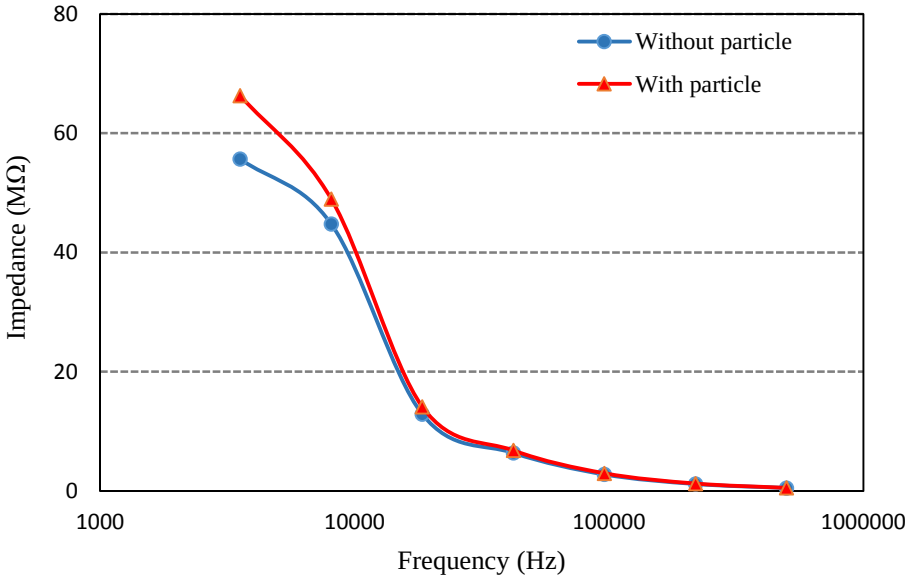

Figure 4.12: Impedance measurement results of polystyrene microparticle experiments in DI water at 0.8 V

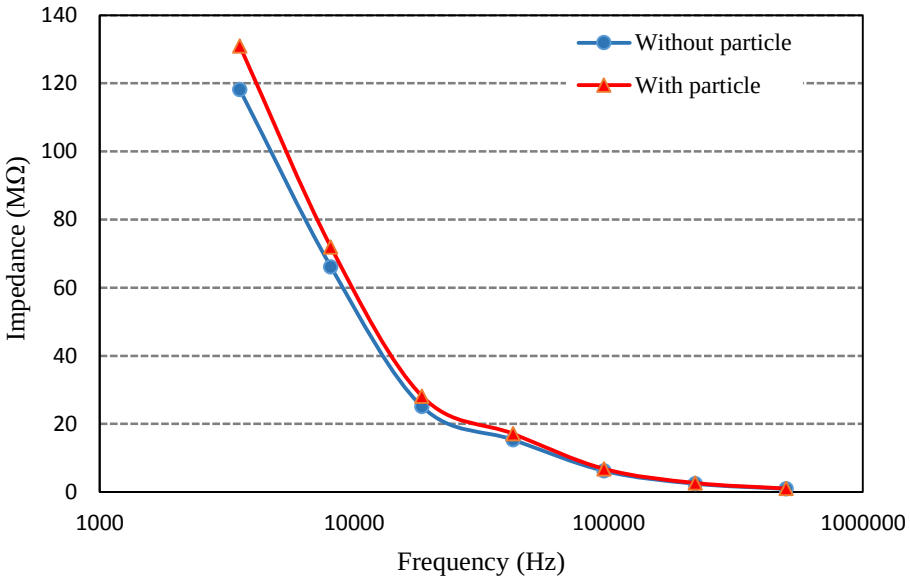

Figure 4.13: Impedance measurement results of polystyrene microparticle experiments in DI water at 1V

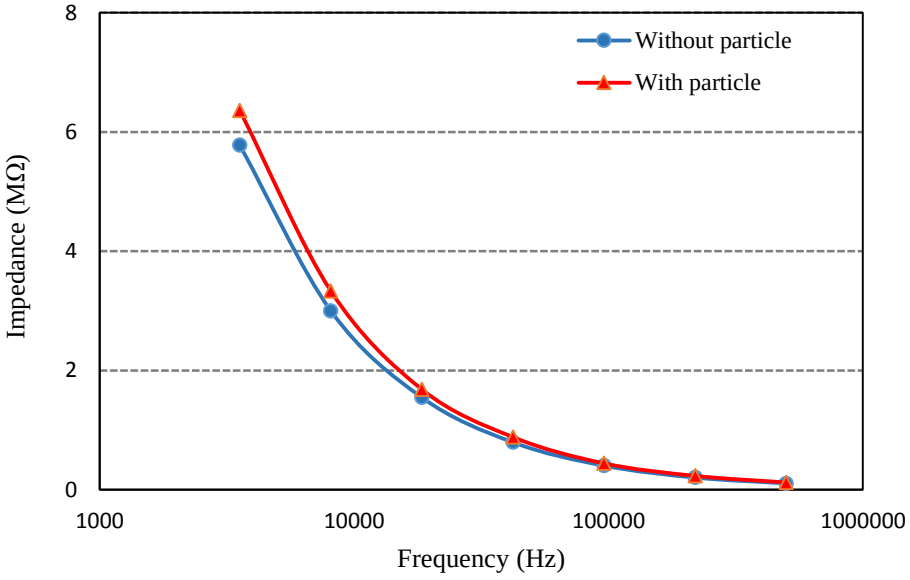

Figure 4.14: Impedance measurement results of polystyrene microparticle experiments in 150 mM NaCl at 0.1 V

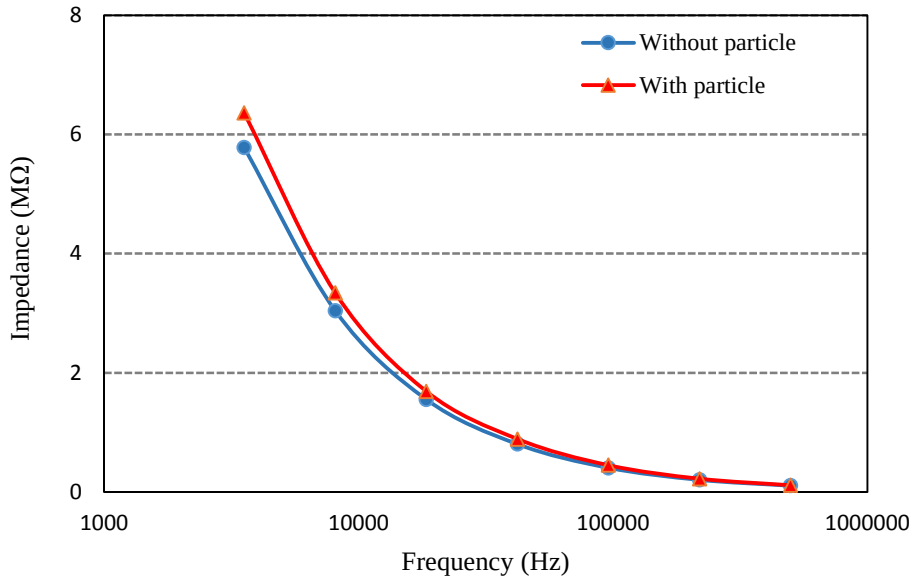

Figure 4.15: Impedance measurement results of polystyrene microparticle experiments in 150 mM NaCl at 0.2 V

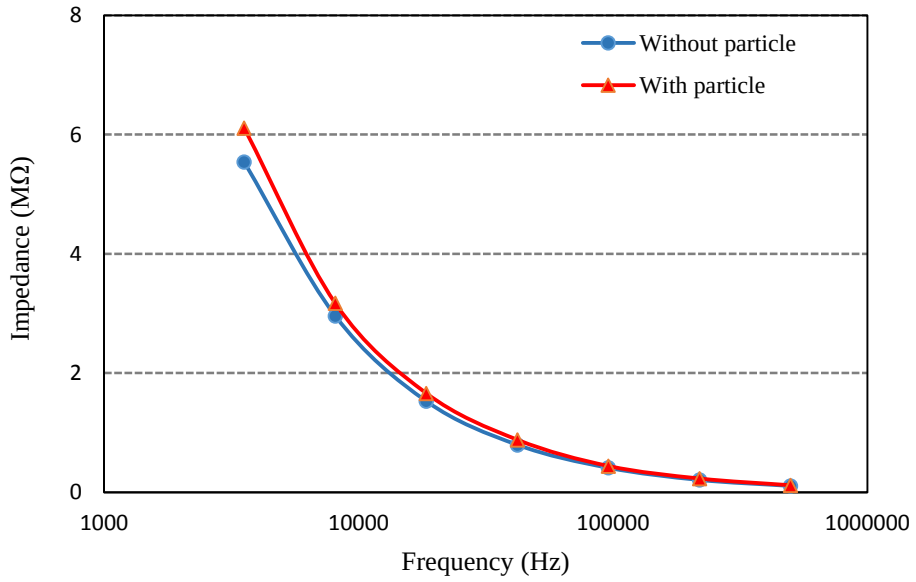

Figure 4.16: Impedance measurement results of polystyrene microparticle experiments in 150 mM NaCl at 0.4 V

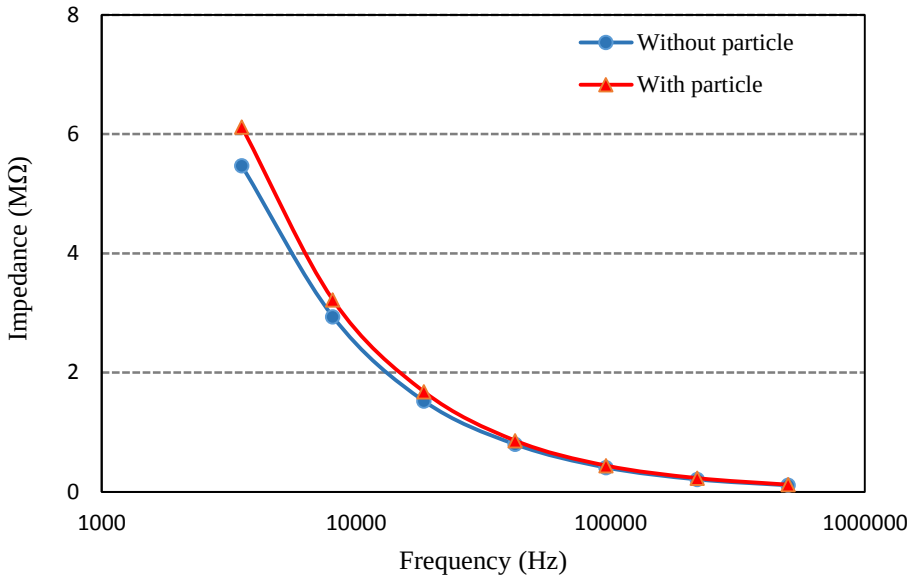

Figure 4.17: Impedance measurement results of polystyrene microparticle experiments in 150 mM NaCl at 0.6 V

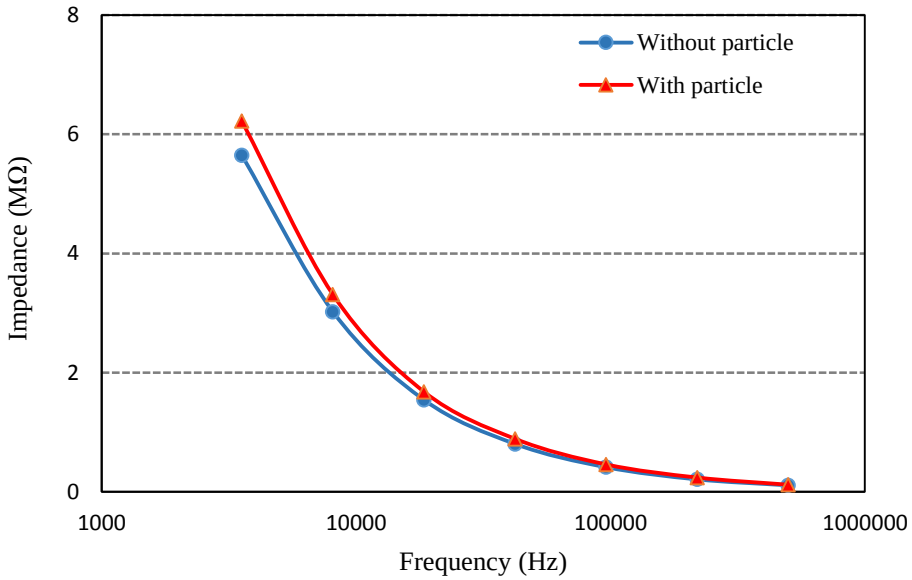

Figure 4.18: Impedance measurement results of polystyrene microparticle experiments in 150 mM NaCl at 1 V

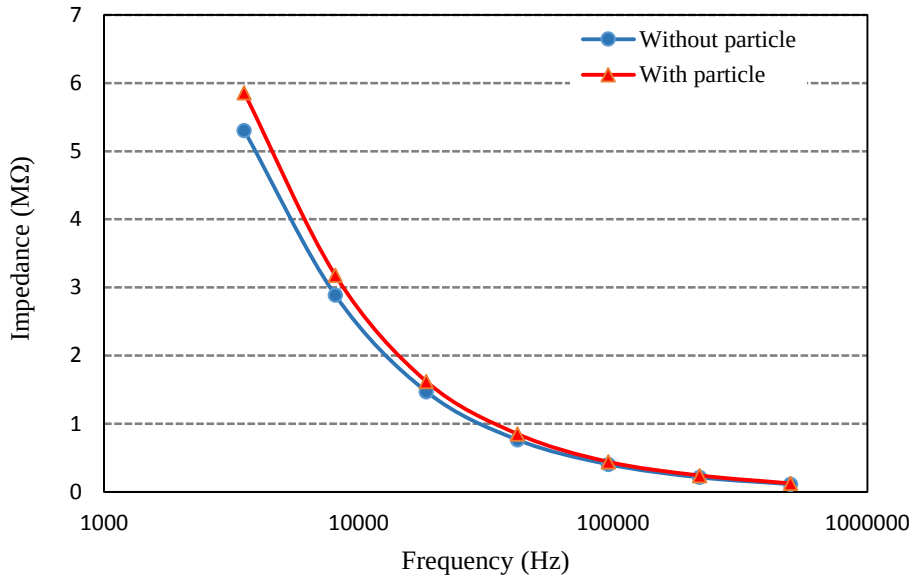

Figure 4.19: Impedance measurement results of polystyrene microparticle experiments in 150 mM NaCl at 2 V

Table 4.12: Impedance increased results in DI water

Frequency (Hz)	Impedance Increased (%)							
	0.2 V	0.4 V	0.6 V	0.8 V	1 V	Max	Min	Mean
3557	10.26	9.16	9.15	10.20	10.84	10.84	9.15	9.92
8111	9.48	7.95	10.56	12.22	8.78	12.22	7.95	9.80
18490	11.79	10.57	11.86	9.79	12.15	12.15	9.79	11.23
42170	9.52	10.37	8.51	11.37	11.42	11.42	8.51	10.24
96160	13.36	12.55	9.32	7.65	9.42	13.36	7.65	10.46
219300	7.61	12.01	8.71	10.19	9.23	12.01	7.61	9.55
500000	7.74	12.22	6.17	10.15	12.15	12.22	6.17	9.69

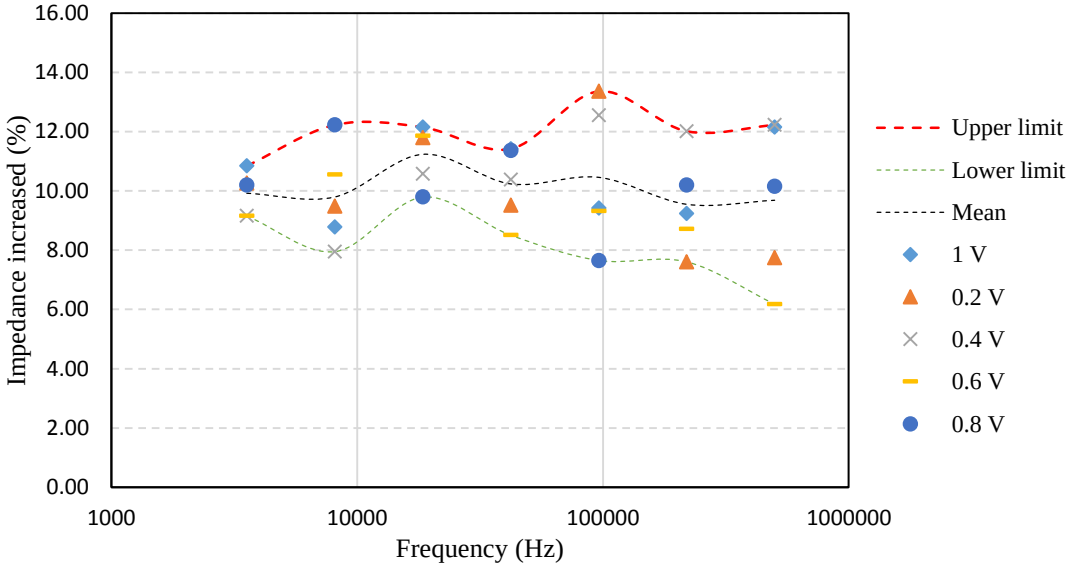

Figure 4.20: Upper limit, lower limit and mean curves of impedance increased in DI water

Table 4.13: Impedance increased results in Nacl

Frequency (Hz)	Impedance Increased (%)								
	0.1 V	0.2 V	0.4 V	0.6 V	1 V	2 V	Max	Min	Mean
3557	10.09	10.05	10.31	11.90	10.15	10.45	11.90	10.05	10.49
8111	11.10	9.84	7.15	9.59	9.53	10.12	11.10	7.15	9.55
18490	8.79	8.75	8.72	10.33	8.84	10.09	10.33	8.72	9.26
42170	10.97	10.66	10.71	7.85	10.63	11.28	11.28	7.85	10.35
96160	9.61	10.68	7.38	8.00	11.18	9.09	11.18	7.38	9.32
219300	13.82	9.26	11.48	10.46	14.47	13.04	14.47	9.26	12.09
500000	15.06	6.95	9.86	10.18	9.52	10.31	15.06	6.95	10.31

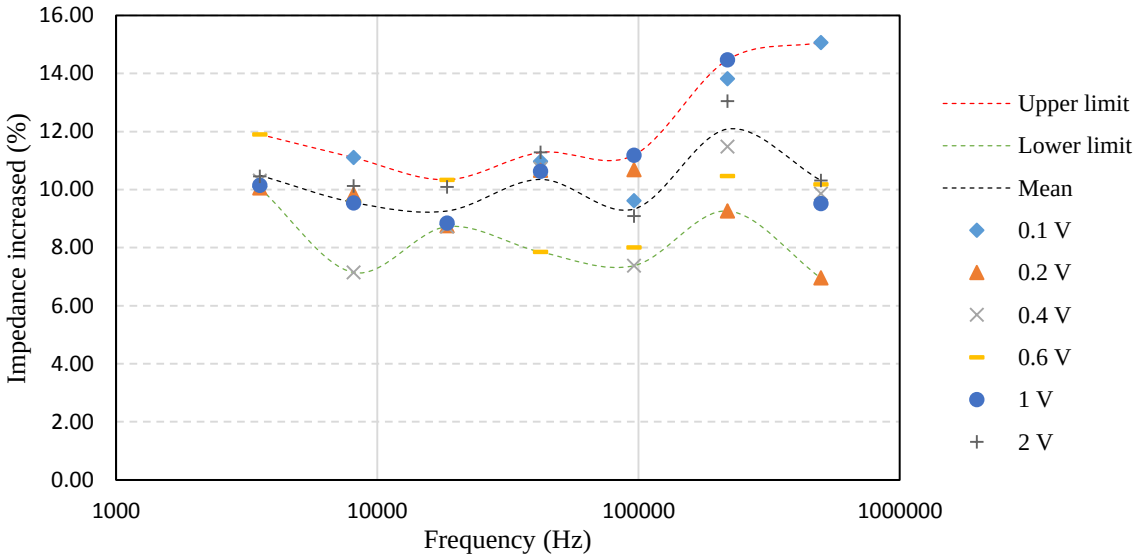

Figure 4.21: Upper limit, lower limit and mean curves of impedance increased in Nacl

5. CONCLUSION AND FUTURE WORK

5.1 Conclusion and Discussion

The goal of this project was to capture a single particle from solution and take an impedance measurement of it in order to obtain information about its properties. To achieve this goal the electrodes and micochannel structures designed using Ledit (v13) and the mask for each of them was written by laser writer. The standard photolithograpy technology and lift off process used to obtain the electrodes on the glass pattern. Photolithography is a process used in microfabrication to pattern a substrate. It uses light to transfer a geometric pattern from a photomask to a light-sensitive chemical photoresist**.** In lift-off processes a sacrificial material, such as photoresist, is first deposited and patterned on the substrate. The material of interest is then deposited on top and the sacrificial material is subsequently removed, leaving behind only the material deposited directly on the substrate. The metal layer which was Titanium in this study deposited using the electron beam physical vapor deposition on the glass substrate. For microchannel a Poly-di-methyl-siloxane (PDMS) chip was created using photolithography to define the channel region and then making PDMS, pouring it into mold structure, curing it and finally peeling it off from the substrate mold. The completed PDMS structure was bonded with the glass substrate after surface treatment by using oxygen plasma cleaner. The chip is composed of trapping chambers connected to the main channel, DEP or actuation electrodes, and sensing electrodes. First, particles introduced into inlet and move through main channel. When a particle arrives to actuation electrodes, it is forced into trapping chamber by negative DEP. The impedance detection is related to the electrode response to the application of a periodic alternating current (AC) signal.

Impedance detection that uses sensing electrodes in an aqueous solution modeled as a simple electrical circuit without the particle and with a particle. Then, trapping of the particle electrically monitored by measuring the impedance change at sensing electrodes after the positioning of the particle between two sensing electrodes. The drain channel design and sensing electrodes placed in the trapping chamber allowed electrical monitoring of single-particle isolation into desired locations.

As it is explained in the result chapter, the impedance was measured at different voltages ranges (0.1-2 V) between 3 KHz and 500 KHz for two different solutions, DI water and 150mM NaCl. The impedance was measured before and after trapping a polystyrene particle and an increasement observed. The impedance increase can be explained by a gradual blockage of the electrical path between the sensing electrodes. Also as it was explained in the electrical model, after placing the particle between sensing electrodes the resistance of particle results a higher impedance. The impedance measurement over wide frequency range done and revealed that the impedance decreased as the frequency increased. This outcome also can be explained due this theory that with increasing the frequency, the double-layer capacitance on each electrode will be decreased and make the impedance lower. In addition, the increment ratio was more evident for the particle experiment and the low frequency. Also it is obvious that with increasing the voltage, it was a slight decrease in impedance in most of frequencies. Furthermore comparison of the obtained results for DI water and 150mM NaCl shows less impedance magnitudes for 150mM NaCl which can be described due to increase of the conductivity of the suspending medium for different frequencies and at different voltages. Although different solutions are used for impedance evaluation of polystyrene particles, results in both case are close to each other with approximately 10% increasing.

5.2 Future Work

The next step would be to use the system to capture a single live particle and measure impedance. Different kind of cancer cells can be distinguished by this method as they show different magnitude and phase. The reason is due to differences between individual cells such as the surface proteins on the cell membrane, the ions concentration in the cytoplasm, cell size and so on. These differences may result in discrepant conductivity and permittivity in various cells. Also a modification in the geometry of electrodes and microchannel would be helpful to get more accurate results. Another improvement would be to find an easier, more reliable method of bonding the PDMS chamber to the glass wafer so that the electrodes are aligned to the chamber without having to manually align them before the plasma treatment expires. Further work could be done to better measure the phase values (which for this study were ignored due to large noise that could not be filtered out) to even further characterize particle responses which requires further improvements and more experimental studies.

References

Ashkin, A., Schütze, K., Dziedzic, J. M., Euteneuer, U., & Schliwa, M. (1990). Force generation of organelle transport measured in vivo by an infrared laser trap.

Bakewell, D. J., Hughes, M. P., Milner, J. J., & Morgan, H. (1998). Dielectrophoretic Manipulation of avidin and DNA. In Proceedings of the 20th Annual International Conference of the IEEE Engineering in Medicine and Biology Society (Vol. 20, No. 2, pp. 1079-1082).

Castellanos, A., Ramos, A., Gonzalez, A., Green, N. G., & Morgan, H. (2003). Electrohydrodynamics and dielectrophoresis in microsystems: scaling laws. Journal of Physics D: Applied Physics, 36(20), 2584.

Chapman, D.L., (1913). Philosophical Magazine, 6, 25, 475.

Chen, N. C., Chen, C. H., Chen, M. K., Jang, L. S., & Wang, M. H. (2014). Single-cell trapping and impedance measurement utilizing dielectrophoresis in a parallel-plate microfluidic device. Sensors and Actuators B: Chemical, 190, 570-577.

Curtis, J. E., Koss, B. A., & Grier, D. G. (2002). Dynamic holographic optical tweezers. Optics Communications, 207(1), 169-175.

Ferrier, G. A., Hladio, A. N., Thomson, D. J., Bridges, G. E., Hedayatipoor, M., Olson, S., & Freeman, M. R. (2008). Microfluidic electromanipulation with capacitive detection for the mechanical analysis of cells. Biomicrofluidics, 2(4), 044102.

Ferrier, G. A., Romanuik, S. F., Thomson, D. J., Bridges, G. E., & Freeman, M. R. (2009). A microwave interferometric system for simultaneous actuation and detection of single biological cells. Lab on a Chip, 9(23), 3406-3412.

Fidler, N., & Fernandez, J. M. (1989). Phase tracking: an improved phase detection technique for cell membrane capacitance measurements. Biophysical journal, 56(6), 1153-1162.

Fortina, P., Surrey, S., & Kricka, L. J. (2002). Molecular diagnostics: hurdles for clinical implementation. Trends in Molecular Medicine, 8(6), 264-266.

Gawad, S., Cheung, K., Seger, U., Bertsch, A., & Renaud, P. (2004). Dielectric spectroscopy in a micromachined flow cytometer: theoretical and practical considerations. Lab on a Chip, 4(3), 241-251.

Giaever, I., & Keese, C. R. (1992). Toxic? Cells can tell. Chemtech, 22(2), 116-125.

Gilchrist, K. H., Giovangrandi, L., & Kovacs, G. T. (2001). Analysis of microelectrode-recorded signals from a cardiac cell line as a tool for pharmaceutical screening. Transduc. Eurosens. 1D3. P, 19, 390-393.

Gilchrist, K. H., Giovangrandi, L., Whittington, R. H., & Kovacs, G. T. (2005). Sensitivity of cell-based biosensors to environmental variables. Biosensors and Bioelectronics, 20(7), 1397-1406.

Gonzalez, A., Ramos, A., Morgan, H., Green, N. G., & Castellanos, A. (2006).

Electrothermal flows generated by alternating and rotating electric fields in microsystems. Journal of Fluid Mechanics, 564, 415-433.

Gouy, G., (1909). Comtes Rendus of the French Academy of Sciences, 149,654,1910, Journal of Physics, 4, 9, 457.

Graf, T., & Stadtfeld, M. (2008). Heterogeneity of embryonic and adult stem cells. Cell Stem Cell, 3(5), 480-483.

Green, N. G., Ramos, A., González, A., Castellanos, A., & Morgan, H. (2001). Electrothermally induced fluid flow on microelectrodes. Journal of Electrostatics, 53(2), 71-87.

Heida, T., Rutten, W. L., & Marani, E. (2001). Dielectrophoretic trapping of dissociated fetal cortical rat neurons. Biomedical Engineering, IEEE Transactions on, 48(8), 921-930.

Heida, T., Rutten, W. L. C., & Marani, E. (2002). Understanding dielectrophoretic trapping of neuronal cells: modelling electric field, electrode-liquid interface and fluid flow. Journal of Physics D: Applied Physics, 35(13), 1592.

Hochmuth, R. M. (2000). Micropipette aspiration of living cells. Journal of Biomechanics, 33(1), 15-22.

Hong, J. L., Lan, K. C., & Jang, L. S. (2012). Electrical characteristics analysis of various cancer cells using a microfluidic device based on single-cell impedance measurement. Sensors and Actuators B: Chemical, 173, 927-934.

Hunt, T. P., & Westervelt, R. M. (2006). Dielectrophoresis tweezers for single cell manipulation. Biomedical microdevices, 8(3), 227-230.

Ichiki, T., Shinbashi, S., & Ujiie, T. (2002). Microchip technologies for the analysis of biological cells. Journal of Photopolymer Science and Technology, 15(3), 487-492.

Irish, J. M., Kotecha, N., & Nolan, G. P. (2006). Mapping normal and cancer cell signalling networks: towards single-cell proteomics. Nature Reviews Cancer, 6(2), 146-155.

Jang, L. S., & Wang, M. H. (2007). Microfluidic device for cell capture and impedance measurement. Biomedical microdevices, 9(5), 737-743.

Jang, L. S., Huang, P. H., & Lan, K. C. (2009). Single-cell trapping utilizing negative dielectrophoretic quadrupole and microwell electrodes. Biosensors and Bioelectronics, 24(12), 3637-3644.

Jones, T. B. (2005). Electromechanics of particles. Cambridge University Press.

Kwong, C. C., Li, N., & Ho, C. M. (2005, November). Studies of deionization and impedance spectroscopy for blood analyzer. In Optics East 2005 (pp. 60030N-60030N). International Society for Optics and Photonics.

Lennon, E., Ostrovidov, S., Senez, V., & Fujii, T. (2006, May). Dielectrophoresis, cell culture, and electrical impedance spectroscopy applied to adherent cells in a single

biochip. In Microtechnologies in Medicine and Biology, 2006 International Conference on (pp. 165-168). IEEE.

Le Pioufle, B., Surbled, P., Nagai, H., Murakami, Y., Chun, K. S., Tamiya, E., & Fujita, H. (2000). Living cells captured on a bio-microsystem devoted to DNA injection. Materials Science and Engineering: C, 12(1), 77-81.

Lian, M., Islam, N., & Wu, J. (2007). AC electrothermal manipulation of conductive fluids and particles for lab-chip applications. IET Nanobiotechnology, 1(3), 36-43.

Manaresi, N., Romani, A., Medoro, G., Altomare, L., Leonardi, A., Tartagni, M., & Guerrieri, R. (2003). A CMOS chip for individual cell manipulation and detection. Solid-State Circuits, IEEE Journal of Solid-State Circuits, 38(12), 2297-2305.

Morgan H, Hughes MP, and Green NG (1999). Separation of Sub-Micron Particles by Dielectrophoresis. Biochip Journal, 77, 516-525.

Morgan, H., Holmes, D., & Green, N. (2005, July). High speed simultaneous optical and impedance analysis of single particles. In Microtechnologies for the New Millennium 2005 (pp. 263-272). International Society for Optics and Photonics.

Muys, J., Alkaisi, M. M., Evans, J. J., & Nagase, J. (2005). Biochip: cellular analysis by atomic force microscopy using dielectrophoretic manipulation. Japanese journal of applied physics, 44(7S), 5717.

Niikura, M., Maeda, A., Ikegami, T., Saijo, M., Kurane, I., & Morikawa, S. (2004). Modification of endothelial cell functions by Hantaan virus infection: prolonged hyper-permeability induced by TNF-alpha of hantaan virus-infected endothelial cell monolayers. Archives of virology, 149(7), 1279-1292.

Pohl, H. A. (1951). The motion and precipitation of suspensoids in divergent electric fields. Journal of Applied Physics, 22(7), 869-871.

Pohl, H. A., & Pollock, K. (1978). Electrode geometries for various dielectrophoretic force laws. Journal of Electrostatics, 5, 337-342.

Ramos, A., Morgan, H., Green, N. G., & Castellanos, A. (1998). AC electrokinetics: a review of forces in microelectrode structures. Journal of Physics D: Applied Physics, 31(18), 2338.

Revzin, A., Sekine, K., Sin, A., Tompkins, R. G., & Toner, M. (2005). Development of a microfabricated cytometry platform for characterization and sorting of individual leukocytes. Lab on a Chip, 5(1), 30-37.

Rosenthal, A., & Voldman, J. (2005). Dielectrophoretic traps for single-particle patterning. Biophysical Journal, 88(3), 2193-2205.

Sabounchi, P., Morales, A. M., Ponce, P., Lee, L. P., Simmons, B. A., & Davalos, R. V. (2008). Sample concentration and impedance detection on a microfluidic polymer chip. Biomedical microdevices, 10(5), 661-670.

Schnelle, T., Hagedorn, R., Fuhr, G., Fiedler, S., and Muller, T., (1993). "3-Dimensionalelectric-field traps for manipulation of cells: calculation and experimental verification," Biochimica et Biophysica Acta, 1157, 127-140.

Suehiro, J., Ohtsubo, A., Hatano, T., & Hara, M. (2006). Selective detection of bacteria by a dielectrophoretic impedance measurement method using an antibody-immobilized electrode chip. Sensors and Actuators B: Chemical, 119(1), 319-326.

Sun, T., Green, N. G., & Morgan, H. (2008). Analytical and numerical modeling methods for impedance analysis of single cells on-chip. Nano, 3(01), 55-63.

Taff, B. M., & Voldman, J. (2005). A scalable addressable positive-dielectrophoretic cell-sorting array. Analytical chemistry, 77(24), 7976-7983.

Voldman, J., Braff, R. A., Toner, M., Gray, M. L., & Schmidt, M. A. (2001). Holding forces of single-particle dielectrophoretic traps. Biophysical Journal, 80(1), 531-542.

Voldman, J., Toner, M., Gray, M. L., & Schmidt, M. A. (2003). Design and analysis of extruded quadrupolar dielectrophoretic traps. Journal of electrostatics, 57(1), 69-90.

Wang, D., & Bodovitz, S. (2010). Single cell analysis: the new frontier in 'omics'. Trends in biotechnology, 28(6), 281-290.

Wu, L. Y., Di Carlo, D., & Lee, L. P. (2008). Microfluidic self-assembly of tumor spheroids for anticancer drug discovery. Biomedical microdevices, 10(2), 197-202.

Yang, J., Huang, Y., Wang, X. B., Becker, F. F., & Gascoyne, P. R. (2000). Differential analysis of human leukocytes by dielectrophoretic field-flow-fractionation. Biophysical Journal, 78(5), 2680-2689.

Yasukawa, T., Suzuki, M., Sekiya, T., Shiku, H., & Matsue, T. (2007). Flow sandwich-type immunoassay in microfluidic devices based on negative dielectrophoresis. Biosensors and Bioelectronics, 22(11), 2730-2736.

Ye, L., Martin, T. A., Parr, C., Harrison, G. M., Mansel, R. E., & Jiang, W. G. (2003). Biphasic effects of 17-β-estradiol on expression of occludin and transendothelial resistance and paracellular permeability in human vascular endothelial cells. Journal of cellular physiology, 196(2), 362-369.

Yu, Z., Xiang, G., Pan, L., Huang, L., Yu, Z., Xing, W., & Cheng, J. (2004). Negative dielectrophoretic force assisted construction of ordered neuronal networks on cell positioning bioelectronic chips. Biomedical microdevices, 6(4), 311-324.

Zou, Z., Lee, S., & Ahn, C. H. (2008). A polymer microfluidic chip with interdigitated electrodes arrays for simultaneous dielectrophoretic manipulation and impedimetric detection of microparticles. Sensors Journal, IEEE, 8(5), 527-535.

GOLEZAR GILANIZADEHDIZAJ

Contact Information:

DOB: 07/04/1985

Address: Emniyetevler Mh., Berrak Sk., NO:10/8,
Kagithane, Istanbul, Turkey
Cell Phone: (+90)5319360594
Email: golzar.g1985@gmail.com
gilanizadedizaj@itu.edu.tr

Education:

2005-2010: BSc of Mechanical Engineering (Heat & Fluids), Department of Mechanical Engineering, Urmia University, Urmia, Iran

- **Dissertation Title:** Composite Materials (FGM)
- **Supervisor:** Assis. Prof. Dr. Rash Ahmadi

2012-present: MSc Student at Nano science and Nano engineering,
Graduate School of Science and Technology, Istanbul Technical University, Istanbul, Turkey
Thesis Title: Single Particle Impedance Measurement Using a Microfluidic Chip,

- **Supervisor:** Assoc. Prof. Dr. Hüseyin Kizil
- **GPA:** 3.69

Research Interest:

- MEMS (Micro Electro Mechanical Systems)
- Lab on a Chip
- Dielectrophoresis
- Microfluidics

Papers:

1. Safari MJS, Mohammadi M, Manafpour M and **Gilanizadehdizaj G,** (2011). "Incipient deposition of sediment particles in rigid boundary channels with circular, rectangular and U-shaped cross sections", *Proceeding of 10th International Hydraulic Conference,* 8-10 November, University of Guilan, Rasht, Iran.

2. Safari MJS, Mohammadi M and **Gilanizadehdizaj G,** (2013) "Experimental Study on incipient motion and deposition of sediment particles in rigid boundary channels" *Water and Soil Science*. 23(3), 13-24.

3. Safari MJS, Mohammadi M and **Gilanizadehdizaj G,** (2014) "On the effect of cross sectional shape on incipient motion and deposition of sediments in fixed bed channels". *Journal of Hydrology and Hydromechanics,* 62(1), 75-82.

Professional Activities:

- **2009**: Tabriz Tractor Manufacturing Factory. Internship

- **2011**: Control Manager of ShahryaranChichest Company, Current Project: Urmia City Hall's "Construction Police" project.

Conferences Attendance:

- **2011:** Certificate for presentation and cooperation with the 10th Iranian Hydraulic Conference, University of Guilan, Rasht, Iran, 8-10 November.
- **2013:** Attended to ITU Nano-TR Student conference (22 September).
- **2013:** Attended to WORKSHOP for Writing and Presenting Research organized by Editage in association with Istanbul Technical University (26 November)
- **2014:** Attended to 25th MicroMechanics Europe (MME) organized by ITU-MEMS in Istanbul (31 August and 1_3 September)

Memberships:

- Permanent member of "Construction Engineering Organization of West Azerbaijan", Iran.

Research Experience:

- **2011-2012:** Sediment Transport in Open Channel Flow, Urmia University. Urmia. Iran.
- **2013-2014:** Full time work at MEMS laboratory of Istanbul Technical University on My Thesis

Skills:

- **Spoken Languages**: English (IELTS 6.5), Farsi (National Language), Turkish,
- **General Software**: Windows (98+, 2000, NT, XP+, 7, 8), Microsoft Office (Word, Excel, PowerPoint)
- **Engineering Software**: COMSOL Multiphysics, L-edit, *LayoutEditor*

References:

- **Hüseyin Kızıl**
  Associate Professor of Metallurgical and Materials Engineering Department,
  Faculty of Chemical and Metallurgical Engineering, Istanbul Technical University,
  Email: kizilh@itu.edu.tr , Tel: +90(212) 285 3516

- **Levent Trabzon**
  Professor of Mechanical Engineering Department, Faculty of Mechanical Engineering, Istanbul Technical University, Email: levent.trabzon@itu.edu.tr, Tel: (+90 212) 293 1300

- **Mirali Mohammadi**
  Associate Professor of Civil Engineering Department, Urmia University,
  Email: m.mohammadi@urmia.ac.ir, Tel: +98 (914) 146 3202